

THE EFFECT OF METAL DOPING ON TiO₂ FOR PHOTOCATALYTIC APPLICATIONS

**A Thesis Submitted to
the Graduate School of Engineering and Sciences of
İzmir Institute of Technology
in Partial Fulfillment of the Requirements for the Degree of**

MASTER OF SCIENCE

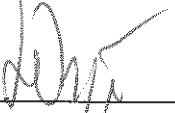
in Biotechnology

**by
Yeşim Alduran**

**July 2019
İZMİR**

We approve the thesis of Yeşim ALDURAN

Examining Committee Members:



Prof. Dr. Lütfi ÖZYÜZER
Department of Physics, İzmir Institute of Technology



Assoc. Prof. Dr. Engin ÖZÇİVİCİ
Department of Bioengineering, İzmir Institute of Technology



Prof. Dr. Aysun AKŞİT
Department of Textile Engineering, 9 Eylül University

01 July 2019



Prof. Dr. Lütfi ÖZYÜZER
Supervisor, Department of Physics
İzmir Institute of Technology



Prof. Dr. Orhan ÖZTÜRK
Co-Supervisor, Department of Physics
İzmir Institute of Technology



Assoc. Prof. Dr. Engin ÖZÇİVİCİ
Head of the Programme of Biotechnology
and Bioengineering



Prof. Dr. Aysun SOFUOĞLU
Dean of the Graduate School of
Engineering and Sciences

ACKNOWLEDGMENTS

Firstly, I would like to thank my supervisor Prof. Dr. Lütfi ÖZYÜZER for his comprehensive supports, encourages and his valuable time and experiences that he patiently shared during my days in this research, and also many thanks to Prof. Dr. Gülnur AYGÜN for her permanent cares, morally supports and her valuable advices.

I wish to thank the thesis committee members Assoc. Prof. Dr. Engin ÖZÇİVİCİ and Prof. Dr. Aysun AKŞİT for their interest, sincerity and participation and valuable comments.

My deep thanks to my dear instructor Dr. Mehtap ÖZDEMİR KÖKLÜ who provided information about my experimental studies, theoretical information and solutions. She helped to shape my master's thesis and provided me for whatever I needed.

I would also like to thank the TUBITAK 117M741 project that supported me throughout my work. This work is also partially supported by Teknoma Technological Materials Industrial and Trading Inc.

I also would like to thank my best friend Zemzem UYANIK who was always near to me with her fruitfully supports since my undergraduate level up to now and I am sure it is not the end. I appreciate of all the group members Aileen NOORI, Bengü ATA, Merve EKMEKÇİOĞLU, José Enrique MARTÍNEZ MEDİNA and rest of Özyüzer Research Group members and Physics department research assistants Koray KAYMAZLAR and Kemal GULTEKIN for their help and friendship throughout my thesis study. I want to espeically thank to my fiance Salih HOCAOĞLU for his support, patience and endless love throughout my recent years.

Finally, but not least I would like to thank my beloved parents for their understanding and encouragements in all of my life's moments.

ABSTRACT

THE EFFECT OF METAL DOPING ON TiO₂ FOR PHOTOCATALYTIC APPLICATIONS

Recently, the photocatalysis method has been an active research area as a promising solution for environmental cleaning method, leading to self-cleaning and sterilization of solar cell surfaces to produce water dissociation reaction. Titanium dioxide (TiO₂) is the most suitable semiconductor for photocatalytic applications due to its high oxidation potential and high efficiency when irradiated by ultraviolet light (UV).

Undoped and Ruthenium (Ru⁺) doped TiO₂ thin films were prepared using magnetron sputtering technique. All thin films were grown on SLG different ratios like 1 sec, 3 secs, 5 secs and 7 secs to set shutter position in magnetron sputter target. Transparent substrate SLG is coated with nearly 50 nm TiO₂ thin films without compromising any optical properties. Samples were heat treated for two hours at 500°C to get the anatase phase crystal structure. The crystallization peaks of TiO₂ are proved to get the anatase phase. Photocatalytic activity of TiO₂ thin films are determined after 1, 3, 5 and 24 hours with organic pollution as a methylene blue dye degradation under UV light. The degradation of methylene blue was investigated kinetically and photocatalytic activity rate constants of the photocatalysts were calculated. All thin films could not reach super hydrophilicity state. Undoped TiO₂ contact angle 47.309° and Ru doped TiO₂ 63.218° were evaluated. The photocatalytic degradation percentage of Methylene Blue was reached 87%, after 24 hours of UV irradiation, when using Ru-doped TiO₂ thin film. Consequently, the anatase phase of Ru-doped TiO₂ thin films are found best photocatalytic activity in self-cleaning performance.

ÖZET

FOTOKATALİTİK UYGULAMALARDA METAL KATKILAMANIN TiO₂ ÜZERİNDEKİ ETKİSİ

Son yıllarda, çevresel temizleme yöntemleri arasında umut verici bir çözüm olarak aktif bir araştırma alanına sahip olan fotokataliz yöntemi, suyun ayrışma mekanizmasını kullanarak güneş panellerinin üst yüzeylerinin kendi kendini temizlemesini sağlamada kullanılan bir uygulamadır. Titanyum dioksit (TiO₂), ultraviyole ışık (UV) ile uyarıldığında yüksek verimliliği ve oksidasyon potansiyeli nedeniyle fotokatalitik uygulamalar için en uygun yarı iletkenidir.

Fotokatalitik aktiviteyi iyileştirmek için farklı oranlarda Rutenyum (Ru⁺) metal iyonları TiO₂ ince film içerisine katkılındı. TiO₂ ince filmler miknatıssal saçırma yöntemi kullanılarak hazırlandı. Miknatıssal saçırma kaynağı üzerindeki kapağın pozisyonu ayarlanarak Ru⁺ iyonları 1, 3, 5 ve 7 saniye boyunca TiO₂ ince film içerisine katkılındırıldı. Yaklaşık 50 nm kalınlığında ince filmler, optik özelliklerini kaybetmeden SLG üzerine kaplandı. Tüm numuneler her kaplama sonrası anataz kristal fazını elde edebilmek için iki saat boyunca 500 °C'de ısıl işleme tabi tutuldu. TiO₂'nin 1 ve 7 saniye Ru⁺ katkılındırılan ince filmleri kristal pikleri anataz fazının elde edildiğini gösterdi. TiO₂ ince filmlerin fotokatalitik aktivitesi, organik kirlilik olarak metilen mavisi boyasının UV ışık altında 1, 3, 5 ve 24. saat sonunda bozunması incelenerek saptandı. Metilen mavisi çözeltisinin fotokatalitik aktivite sonucu bozunması kinetik olarak incelenip ve fotokatalitik aktivite oranları hesaplandı. TiO₂ ince filmler süperhidroflık duruma ulaşamadı ancak katılanmamış TiO₂ ince filmin temas açısı 47.309° ve Ru katkılı TiO₂ ince filmin temas açısı 63.218° olarak hesaplandı. TiO₂ ince film numunelerinin Metilen Mavisi çözeltisi içerisinde fotokatalitik olarak bozunma yüzdesi, 24 saatlik UV ışınlanmasından sonra, %87'ye ulaştı. Sonuç olarak, Ru⁺ katkılı TiO₂ ince filmlerin anataz fazı, kendi kendini temizleme performansında en iyi fotokatalitik aktiviteye sahip olduğu ispatlandı.

To my family...

TABLE OF CONTENTS

LIST OF FIGURES.....	ix
LIST OF TABLES.....	xi
CHAPTER 1 INTRODUCTION	1
1.1. General Information.....	1
1.2. The Aim of the Thesis	4
CHAPTER 2 THEORETICAL BACKGROUND.....	5
2.1. Importance of Photocatalyst	5
2.2. TiO ₂ as a Photocatalyst.....	7
2.3. TiO ₂ Band Theory.....	10
2.4. The Mechanism of Action TiO ₂	11
2.5. Cleaning Methods of Solar Panels	15
2.5.1. Natural Methods.....	15
2.5.2. Mechanical Methods	15
2.5.3. Electrostatic Methods	16
2.5.4. Self-Cleaning Methods.....	16
2.5.4.1. Volatile Organic Compounds (VOCs).....	16
2.6. Applications of TiO ₂ Photocatalyst.....	18
2.6.1. Anti-Fogging Effect	19
2.6.2. Water Purifier Effect	20
2.6.3. Air Cleaning Effect	20
2.6.4. Self-Cleaning Effect	21
2.6.5. Anti-Bacterial Effect	21
2.7. Importance of Hydrophilicity	22
2.8. Band Gap Theory of TiO ₂	25
2.9. Enhancement of Photocatalytic Activity of TiO ₂ Thin Films	27
2.9.1. Ruthenium (Ru) doped TiO ₂ Thin Film	28

CHAPTER 3 EXPERIMENTAL PROCEDURE	30
3.1. Growth of Ruthenium (Ru) Doped TiO ₂ Thin Film	30
3.2. Surface Characterization	32
3.3. Photocatalytic Degradation Test of Methylene Blue Dye	33
3.4. Optical Characterization	36
3.5. Phase Characterization	36
3.6. Surface Characterization	37
3.7. Contact Angle Measurement	38
3.8. Surface Resistivity Measurement	38
3.9. Thickness Measurement	39
CHAPTER 4 RESULTS & DISCUSSION	41
4.1. Film Thickness	41
4.2. Optical Characterization	42
4.3. Band Gap Energy	43
4.4. XRD Analysis of Undoped and Doped TiO ₂ Thin Films	47
4.5. Atomic Force Microscopy (AFM) Results	48
4.6. SEM Analysis of Undoped and Ru-doped TiO ₂ Thin Films	50
4.7. Contact Angle Results	55
4.8. Surface Resistivity Measurement	56
4.9. Photocatalytic Activity	57
CHAPTER 5 CONCLUSION	65
REFERENCES	67

LIST OF FIGURES

<u>Figure</u>	<u>Page</u>
Figure 1.1 Some examples of various semiconductor band positions.....	3
Figure 2.1 Comparison of photocatalysis (TiO ₂) and photosynthesis.....	5
Figure 2.2 Absorption area of TiO ₂ in solar spectrum.....	6
Figure 2.3 Crystal structure of anatase, rutile and brookite phase.....	8
Figure 2.4 Band energy diagram of insulators, semiconductors and conductors.....	11
Figure 2.5 Photocatalytic water splitting mechanism.....	15
Figure 2.6 a)Photocatalytic degradation of organic pollutions b)Removal of pollution water due to hydrophilicity of TiO ₂ surface.....	18
Figure 2.7 Photocatalyst Applications.....	19
Figure 2.8 Schematic representation of self-cleaning coated surface.....	21
Figure 2.9 Number of living bacteria on TiO ₂ thin films after irradiation of 30 min interval.....	22
Figure 2.10 Contact angles according to material surface.....	23
Figure 2.11 Schematic representation of photoirradiated hydrophilicity.....	25
Figure 2.12 The process of self-cleaning of TiO ₂ surface with photocatalytic effect.....	25
Figure 2.13 When semiconductor excite with IR radiation, electrons are trapped in shallow state.....	28
Figure 2.14 Schematic illustration of energy level Ruthenium (Ru ⁺) metal doped TiO ₂	29
Figure 3.1 The schematic representation of D.C. Magnetron Sputtering System.....	31
Figure 3.2 Representation of preparation thin film by a D.C. Magnetron Sputtering Technique.....	31
Figure 3.3 Images of Uncoated, Undoped and Ru-doped TiO ₂ Thin Films.....	32
Figure 3.4 Chemical representation of Methylene Blue.....	33
Figure 3.5 Absorbance spectrum of Methylene Blue under several wavelength stimulation.....	33
Figure 3.6 The photocatalytic degradation pathway of methylene blue using a) GC\MS and b) LC\MS.....	34
Figure 3.7 Schematic illustration of photocatalytic activity test experiment with methylene blue solutions.....	35
Figure 3.8 SEM instrument in IZTECH.....	37
Figure 3.9 Contact angle measurement instrument in IZTECH.....	38

<u>Figure</u>	<u>Page</u>
Figure 3.10 Probe 1 and 4 transport current (I), 2 and 3 evaluate voltage (V).....	39
Figure 3.11 Profilometer instrument in IZTECH.....	40
Figure 4.1 Data XY Chart measurement and thickness data of undoped and Ru-doped TiO ₂	41
Figure 4.2 UV-Vis spectrophotometric analysis of uncoated soda lime glass.....	42
Figure 4.3 UV-vis analysis spectrophotometric analysis of undoped and Ru-doped TiO ₂	43
Figure 4.4 Band gap energy of undoped and Ru-doped TiO ₂	44
Figure 4.5 XRD pattern of undoped and Ru doped TiO ₂ thin films samples.....	47
Figure 4.6 2-D and 3-D AFM image for the undoped TiO ₂ thin films and histogram..	48
Figure 4.7 2-D and 3-D AFM image for the Ru doped TiO ₂ thin films and histogram	49
Figure 4.8 (a), (b) and (c) SEM images of undoped TiO ₂ thin films.....	51
Figure 4.9 (a), (b) and (c) SEM images of Ru-doped TiO ₂ thin films.....	52
Figure 4.10 Undoped TiO ₂ thin film EDX spectrums.....	53
Figure 4.11 1s-Ru doped TiO ₂ thin films EDX spectrums.....	54
Figure 4.12 3s-Ru doped TiO ₂ thin films EDX spectrums.....	55
Figure 4.13 5s-Ru doped TiO ₂ thin films EDX spectrums.....	54
Figure 4.14 7s-Ru doped TiO ₂ thin films EDX spectrums.....	55
Figure 4.15 Contact angle results of undoped TiO ₂ and Ru-doped TiO ₂ thin films.....	56
Figure 4.16 Photocatalytic degradation of Methylene Blue solution (10 ⁻⁵ M) with undoped TiO ₂ catalyst.....	57
Figure 4.17 Photocatalytic degradation of Methylene Blue solution (10 ⁻⁵ M) with 1s-Ru doped TiO ₂ catalyst.....	59
Figure 4.18 Photocatalytic degradation of Methylene Blue solution (10 ⁻⁵ M) with 3s-Ru doped TiO ₂ catalyst.....	60
Figure 4.19 Photocatalytic degradation of Methylene Blue solution (10 ⁻⁵ M) with 5s-Ru doped TiO ₂ catalyst.....	61
Figure 4.20 Photocatalytic degradation of Methylene Blue solution (10 ⁻⁵ M) with 7s-Ru doped TiO ₂ catalyst.....	62
Figure 4.21 Absorbance decay of Methylene Blue (MB) solution & UV irradiation time for the undoped and Ru- doped TiO ₂ thin films.....	63
Figure 4.22 ln (A ₀ / A) versus UV irradiation time for the undoped and Ru-doped TiO ₂ thin films.....	64

LIST OF TABLES

<u>Table</u>	<u>Page</u>
Table 2.1 Physical properties of the titanium polymorphs	9
Table 2.2 Reactive species reactions in photocatalysis	13
Table 2.3 Recombination reaction at TiO ₂ photocatalysis	14
Table 2.4 Photocatalytic degradation reaction with any volatile organic compounds ...	14
Table 2.5 Volatile Organic Compounds (VOCs) and Types	17
Table 3.1 Growth parameters of Ru-doped TiO ₂ thin films for D.C magnetron sputtering system.....	32
Table 4.1 Values of the band gap energy of the undoped and Ru doped TiO ₂ thin films samples.....	46
Table 4.2 XRD results of undoped and Ru doped TiO ₂ thin films samples.....	48
Table 4.3 Resistivity values undoped and Ru doped TiO ₂ thin films.....	57
Table 4.4 The values of k (min) ⁻¹ prepared thin films.....	64

CHAPTER 1

INTRODUCTION

Thin film of Titanium Dioxide (TiO_2), which is used as a self-cleaning material. This material will be used for coating the outer of solar panel surface to increase the efficiency and get rid of the accumulation of dust on the solar panel surface. General information about the importance of solar energy have been mentioned, including the historical knowledge is given related to solar panel efficiency and heterogeneous photocatalyst in this dissertation. In theoretical part give an exhaustive explanation of TiO_2 as a specific material which is used as a self-cleaning material with its properties, crystal structure, facts of photocatalysis and importance of hydrophilicity will be identified. The applications of TiO_2 photocatalysis have been clarified as an antifogging effect, water purifier effect, air cleaning effect, antibacterial effect and self-cleaning effect. Afterward, UV photocatalysis mechanism and affecting factors will clarify at the photocatalytic process. The mechanism of hydrophilicity rules and water wettability of (TiO_2) surface is expressed in details. As a consequence, (TiO_2) thin films preparation, investigate doping effect to enhanced photocatalytic activity and the evaluation of photocatalytic activity are explained.

1.1. General Information

It has been notified that worldwide energy consumption has enhanced by 2.2 percent compared to the prior year ("World Energy Statistics"). When non-renewable energy sources are decreasing, solar energy offers as an alternative solution for world's generations. Solar energy systems are useful because they are easy to install and clean, having highest lifetime and durability. Unfortunately, the most main important problem is low efficiency in solar cells energy. Nowadays, the most advanced solar panels efficiency is approximately 20% in the market.

In 1961, two scientists, Shockley and Queisser, discovered silicon-based photovoltaics and the maximum efficiency have been increased by nearly 32% (Cristóbal

López, Martí Vega, and Luque López 2012). All commercial solar panels on the photovoltaic cell which are available in the market have used silicon as the substrate. Nevertheless, silicon-based solar panels too, cannot provide an enough efficiency for the commercial use of the clean energy. By the use of multi-port solar cells, the efficiency can be increased even higher than 32%, but this technique is very expensive so it is not recommended for commercial use.

That's why scientists and investors are looking for new and alternatives techniques to increase efficiency and low cost solution for the commercially use of the solar panels. There are multiple factors to effect directly the efficiency of solar panels such as sunlight intensity, angle of inclination of solar panel and keep cleaning of the surface of the solar panel. The main purpose of this research is to focus on the self-cleaning of the solar panel's surface to increase the efficiency.

Considering the solar panels are established outside of the city previously. However, they have mostly seen that rooftop, car park in the city. Performance of solar panels decrease as the result of high industrialization, volatile organic pollutions for instance dust particles in the air, bird excrement and leaves and urban pollution burning coal and diesel. Any foreign substance on photovoltaic panels influence the sunlight entrance and its converting to the electrical energy in the surface of the solar panels (Ozdemir et al. 2016).

Traditional cleaning methods are insufficient and advanced cleaning methods are very costly for removing such pollutants. Therefore, research on the conversion of toxic substances to harmless components such as carbon dioxide and water have been attracted attention recently. Self-cleaning effect is useful for optically transparent material under UV illumination (Adachi et al. 2018). The method of self-cleaning appears to be a promising method because they are efficient, non-selective, and light-weight.

The technique of photocatalysts have been used in order to break down contaminated particles and organic compounds into the water about 25 years.

A large number of photocatalysts have been reported such as metal-oxides: TiO₂, ZnO, Fe₂O₃, SnO₂, ZrO₂, MgO, SrTiO₃, GeO₂, K₄NbO₁₇, Sb₂O₃, MoO₃, MoS₂, V₂O₅, WO₃, Cu₂O, In₂O₃, Nb₂O₅, ZnFe₂O₄ (H. Pan et al. 2015).

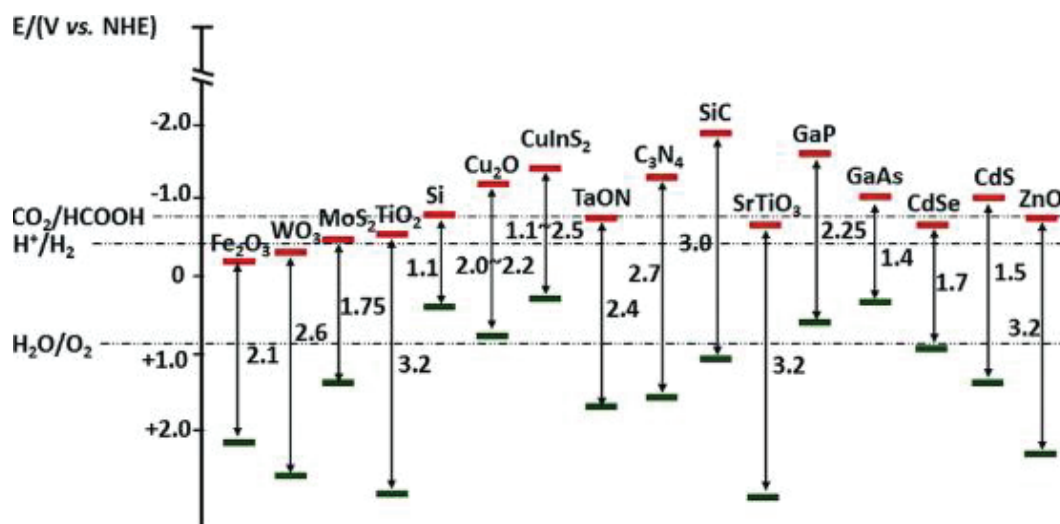


Figure 1.1. Some examples of various semiconductor band positions
(Source: H. Pan et al. 2015).

The photocatalysts which are shown in Figure 1.1. have been used in the degradation of many organic contaminants such as aliphatic or aromatic compounds, dyes, pesticides and herbicides (Malati 2010). Most of these mentioned metal oxides have shown a relatively weak photocatalytic activity respect to TiO_2 (Wenbin, Cao 2016). Due to its strong oxidation ability, chemical stability under UV light, non-toxicity and reasonable price has been determined as the most suitable semiconductor for the photocatalysis.

In the literature, TiO_2 is usually used as powder in a wet process. However, by adding TiO_2 photocatalyst as a particle to the water the following problems have been observed: no homogenous distribution of catalyst throughout the reaction, removal of the catalyst from the medium at the end of each process.

Compared to other conventional methods, TiO_2 thin films that prepared via magnetron sputtering technique shows good mechanical durability, capable of large scale coatings (Karunagaran et al. 2005), applicable for multilayer optical coatings (He et al. 2006), controllable deposition conditions such as heating, mixture of gas flow etc. (Dhayal et al. 2007).

In this thesis, different ratios of undoped and ruthenium doped TiO_2 photocatalysts were produced as a thin film on soda lime glasses (SLG) by magnetron sputtering technique. Essential morphological optimization have been investigated and photocatalytic activity tests have been applied using Methylene Blue dye as an organic contamination.

1.2. The Aim of the Thesis

The main challenge in solar energy as a renewable energy source is the efficiency. Commercially silicon-based solar panels efficiency is around 30% (Masuko et al. 2014).

Today, researchers are trying to obtain higher efficiency result with different techniques but, high efficiency is very expensive. Therefore, it is mandatory to seek for new alternatives inexpensive and more available techniques to increase efficiency and create a commercial use of solar energy. There are some factors that will directly effect on efficiency by decreasing the absorption of solar radiation at a certain rate, including: the installation angle of the solar panels, the amount of dust in the air, panel's surface organic impurities, air water stains, industrial pollution like coal and diesel sources in the environment. These impurities can scratch the solar panel's surface and cause permanent damage to the solar panels and reduce the lifetime of the solar panels.

There are various methods for cleaning solar panels such as naturally, mechanically and electrostatically. However, some of the natural methods including uncontrolled ways like wind energy, rainwater and gravitational effects are not preferable.

Mechanical methods involve using a brush and chemical cleaners can cause irreversible structural damage on the surface. Nevertheless, this is one of the most commonly used methods.

Electrostatic methods are based on the repulsion of similarly charged particles due to that it does not work in rainy weather. For this reason, the self-cleaning method is more effective when compared to others.

The main purpose of this thesis is to focus on the self-cleaning method by improving photocatalytic activities of TiO_2 thin film with doping Ruthenium (Ru^+) metal. This thin film can be used as the upper surface of the solar panels due to its high transparency. In order to clean the surface in more easy way, using the doped TiO_2 thin film, a strong oxidizing environment is created and the organic impurities on the surface are disintegrated and decomposed into the water, carbon dioxide and smaller molecules and finally will be washed by the rain water. This process is kind of self-cleaning technique. In this way, the efficiency of solar panels will be increased by keeping solar absorption at the maximum level.

CHAPTER 2

THEORETICAL BACKGROUND

2.1. Importance of Photocatalyst

Photochemistry is a field which investigates of beam effect between the visible and near ultraviolet region and initiated by absorption of a photon is called photochemical reaction. Some specific photochemical reactions are given specific names (Ibhadon and Fitzpatrick 2013). For examples, photosynthesis is a mechanism which produces oxygen from CO_2 and water using Chlorophyll like a catalyst (Ohama and Van Gemert 2011) Photocatalysis is an opposite mechanism of the photosynthesis. The photocatalyst is a semiconductor material that forms a strongly oxidizing environment on its surface under the influence of ultraviolet (UV) light. When UV light is applied, photocatalyst absorbs light and increases energy. This photon energy is transformed the chemical energy and degrades the microbes, molds, bad odors and produce harmful organic chemicals into carbon dioxide and water by containing high oxidation power (Khan and Adil, 2015).

The process of the photocatalysis and photosynthesis are shown in Figure 2.1. Important advantages of this technology; renewable and provide a good alternative for using pollution-free solar energy treatment method, unlike the transfer of impurities from one side to another like classical treatment method, it produces harmless products (Ibhadon and Fitzpatrick 2013).

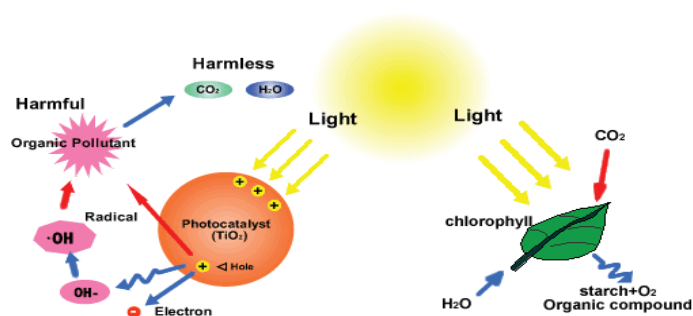


Figure 2.1. Comparison of photocatalysis (TiO_2) and photosynthesis (Source: Kathirvelu, D'Souza, and Dhurai 2008).

The yield of the photocatalyst depends on the wavelength and intensity of the light source. The photocatalyst needs higher energy photon than band energy for activation. Figure 2.2 shows the region where titanium dioxide can absorb in the light spectrum. As can be seen from the figure, this region corresponds to about 5% of the light spectrum. Therefore, a small shift in the band structure can further absorb the solar spectrum and thus increase the performance of the photocatalyst. Similarly, the absence of ultraviolet light in indoor lighting conditions is the biggest obstacle to the use of photocatalyst in closed areas. If the photocatalyst surface area increases, the greater the number of organic substances that will be adsorbed on the surface and thus the activity of the photocatalyst increases. One disadvantage of thin films is that they have a lower surface area than the powder form of TiO_2 . The recombination of electrons and holes in any chemical reaction is the most dominant photocatalytic reaction. Because 95% of the charge carriers (electrons and holes) are recombined without reaction. This situation is the biggest limitation in semiconductor photocatalysis system. The recombination may be on the photocatalyst surface or in the center of the bulk, while the rate of recombination determines the efficiency of the photocatalyst.

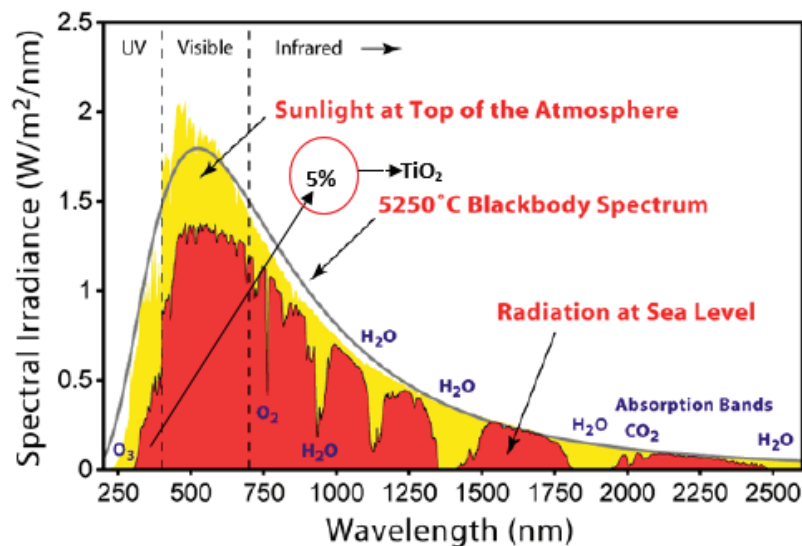


Figure 2.2. Absorption area of TiO_2 in solar spectrum
(Source: Skaaland et al. 2011).

Solar radiation includes different wavelengths of photons. The dispersion of irradiated solar energy has different wavelengths function that is entitled the solar

spectrum. This spectrum contains the ultraviolet (UV), visible (vis) and infrared (IR) wavelength area. As the light radiation passes through the atmosphere, some of the wavelengths are much more affected via absorption and scattering than others. In Figure 2.2. shows the absorption of certain gases and water in the atmosphere in the dip of the curve. The total decline in radiation is clear compared to the spectrum that strikes the outer atmosphere (yellow) and the spectrum that strikes the ground (red) (Skaaland et al. 2011).

2.2. TiO₂ as a Photocatalyst

Titanium dioxide is one of the preferred industrial or consumer materials in our daily life. Titanium is a very rough, silvery white, low corrosion and very bright element. The melting point is 3,020 °F, boiling point 5,949 °F and density is 4,5 g/cm³ at 20 °C. Oxidation states are +2, +3, and +4, as in the oxygen compounds titanium monoxide, TiO, dititanium trioxide, Ti₂O₃, and titanium dioxide, TiO₂, respectively. The +4 oxidation state is the most stable (Britannica 2018).

Titanium dioxide (TiO₂) has three different polymorphs. These are Rutile, Anatase and Brookite. Anatase is the most studied TiO₂ polymorph among the three natural phases (anatase, rutile and brookite) (Pan and Liu 2017). Most common phases are Anatase (3.2 eV 387 nm) and Brookite (3.0 eV 413 nm) (Jagadish 2017). Although, anatase phase of TiO₂ is more toxic than the rutile phase but, when particles become smaller and surface area increase, rutile phase of TiO₂ become harmful. Surface area increase, TiO₂ nanoparticles can absorb UV radiation easily and get great photocatalytic activity. Surface modifications cause changes in photocatalytic activity also (Gurr et al. 2005).

The anatase crystal phase of TiO₂ shows the highest photocatalytic activity than other TiO₂ crystal structures. That's why Anatase type of titanium dioxide is most commonly used as a photocatalyst in the industry (Yoshihiko Ohama and Dionys Van Gemert, 2011). The anatase band gap is higher than rutile. This phase can raise the electron from valence band to conduction band to higher energy levels of the redox potentials of the adsorbed molecules when the absorbable light is low. This case increases the molecule's oxidation power transfer of the electrons and facilitates the transfer of electrons from the TiO₂ to the adsorbed molecules. This statement has also been extended

to illustrate activities related to orientation to the surface, suggesting that different surfaces offer different band gaps.

Anatase electron-hole pair life is longer than rutile for charge carrier in surface reactions. The capture of electrons and holes of the photocatalyst (by molecular oxygen and hydroxyl ion) determines the quantum yield at the surface. On the anatase surface, the holes are joined more tightly than the rutile with the hydroxyl ion. Therefore, the life of the charge carriers of the anatase is higher than that of the rutile. As a result, anatase shows better photocatalytic activity than rutile (Bouhadoun et al. 2017). Rutile is a thermodynamically stable phase between the three natural phases of TiO_2 . Due to its high optical, high chemical stability, high refractive index, high dielectric constant and excellent scattering efficiency, it has a wide range of application areas (J. Pan, Liu, and Liu 2017).

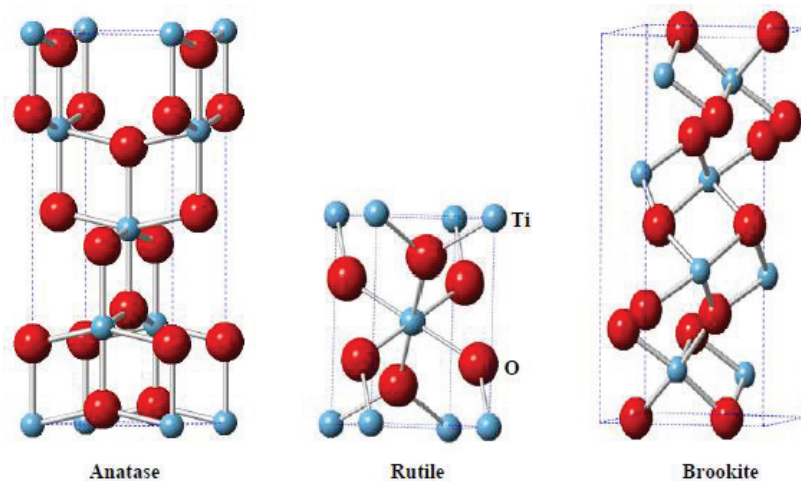


Figure 2.3. Crystal structure of anatase, rutile and brookite phase
(Source: Etacheri, Valentin, and Schneider 2015).

Anatase, rutile and brookite structures can be identified by TiO_6 octahedral chains surrounded by 6 O^{2-} ions octahedral of each Ti^{+4} ions are shown in Figure 2.3. The octahedral in the anatase, rutile and brookite structures are connected by corners, corners edges and edges (Navrotsky, Jamieson, and Kleppa 2008).

The difference between these phases depends on the distortion of the octahedral structures. Rutile structure shows orthorhombic distortion which is not regular. On the other hand, anatase is less distortion than rutile and brookite. The Ti-Ti distances in anatase are more than rutile. However, Ti-O distances in anatase are shorter than rutile.

These differences are reflected in both mass densities and band structures of anatase and rutile (Carp, Huisman, and Reller 2004).

Table 2.1. Physical properties of the titanium polymorphs
(Source: Carp, Huisman, and Reller 2004).

Properties	Anatase	Rutile	Brookite
Crystal Structure	Tetragonal	Tetragonal	Rhombohedral
Density (g/cm ³)	4,26	3,84	4,11
Refractive Index	2,5688	2,9467	2,809
Band Gap (eV)	3,26	3,05	3.2-3.8
Frequency (Hz)	10 ⁴	10 ⁸	-
Dielectric Constant	55	160	-
Lattice Constants (nm)	a= 0,3733 c=0,937	a= 0,4584 c=0,2953	a= 0,5436 c=-
No. of TiO ₂ /unit cell	4	2	8

Photoelectrochemical studies of important inorganic compound TiO₂ were initiated in the late 1960s. Fujishima and Honda (1972) used rutile titanium dioxide (TiO₂) and platinum electrode to separate the water molecule photocatalytically into oxygen and hydrogen (Li and Li 2017). After this discovery, heterogeneous photocatalysis has been started to intense studies against potential environmental pollution problem.

Heterogeneous photocatalysis can be considered as a brightest method in advanced oxidation processes. This process uses molecular oxygen as oxidizing agents and converts impurities into harmless substances. Heterogeneous photocatalysis has been utilized air and water treatment systems, self-cleaning surfaces, solar cells and hydrogen production (Etacheri, Valentin, and Schneider 2015).

Heterogeneous photocatalysis is based on the interaction of semiconductor material with light. The idea of photocatalysis has emerged as the use of solar light as an energy source for environmental cleaning. The heterogeneous photocatalysis method is an ideal and promising approach. Titanium dioxide (TiO₂) is the most commonly studied and used as a photocatalyst among other semiconductors with photocatalytic activity owing to its high oxidation potential, comparatively low cost and high efficiency when irradiated with ultraviolet (UV) light (Vonderhaar 2017). When TiO₂ is irradiated via ultraviolet (UV) light, electron-hole pairs are formed. Electron-hole pairs produce ·OH

radicals and O_2^- super oxides to decompose contaminants on the photocatalyst surface (Ibhadon and Fitzpatrick 2013).

In literature, TiO_2 is used in powder form generally for many applications, whereas there are a lot of essential and practical applications to use it as a thin film. These applications should not be limited to only self-cleaning surfaces or antibacterial surfaces. High-efficiency self-cleaning is important for titanium dioxide-coated self-cleaning surfaces, as well as the commercial success of solar panels in hard-to-reach places and the difficulty cleanliness of larger glass surfaces at high-rise buildings (Pelizzetti and Minero, 2012).

2.3. TiO_2 Band Theory

Semiconductors are the materials between conductor and insulator based on electrical conductivity. These materials which are normally an insulator, when external effects are applied to these substances such as light, heat, electrical stress or magnetic effect, they become conductive by releasing some valence electrons in normal condition. When these external effects are eliminated, they return to the insulator.

Semiconductor materials are characterized by their electronic structures, which are described by "band theory". The band theory defines all substances as a function of electronic energy levels. The materials are classified by the energy gap between these bands.

Insulators have large band gap; that's why a considerable amount of energy must spend to move the electrons from valence band to conduction band to form a current. Conductors have no band gap between a conduction band and valence band. Many electrons can easily shift from valence band to conduction band.

Semiconductors have a small band gap according to insulator that electrons move from the valence band to conduction band to apply any thermal, electrical or light effect from outside. If the light effect that causes the electron to pass from one band to the other, such substances are called photocatalyst. The energy band diagrams of conductors, insulators and semiconductors are shown in Figure 2.4.

When a semiconductor metal oxide absorbs a photon ($h\nu$) equal or greater than the band gap energy, an electron in the valence band passes to the conduction band with femtoseconds of time (Kopidakis 2013). The photonic excitation creates the electron excess (e^-_{CB}) in the conduction band while leaving the electron holes (h^+_{VB}) in the valence

band. Separated electrons and holes can follow different pathways. One possibility is that the electron and hole migrate to the surface of the semiconductor (Li and Li 2017). On the catalyst surface, while the photocatalyst electron is delivered to the electron acceptor (A, generally molecular oxygen), a donor type (D) can be oxidized by the valence band holes. These reactions depend on the valence band and conduction band positions of the semiconductor and also the redox potentials of the adsorbed species (Ibhadon and Fitzpatrick 2013). The recombination of electrons and holes reduces the photocatalytic activity of the semiconductor (the stimulated electron returns to the valence band without reacting with the adsorbed species). Returning electron combines with the hole to release light or heat (Khan and Adil, 2015).

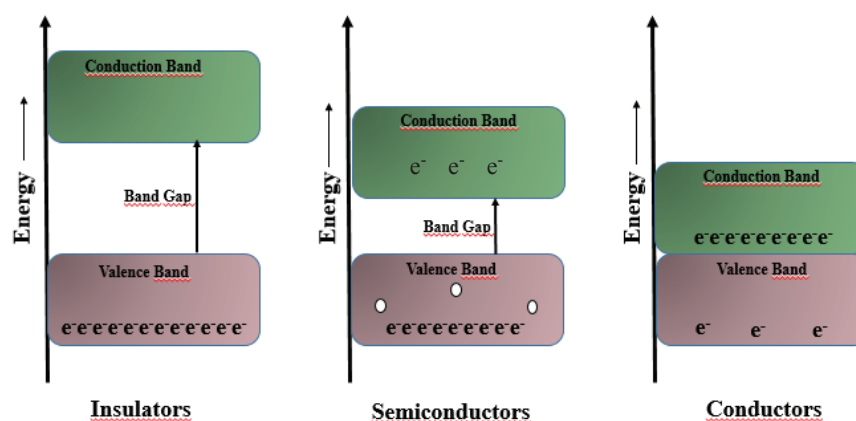


Figure 2.4. Band energy diagram of insulators, semiconductors and conductors

2.4. The Mechanism of Action TiO₂

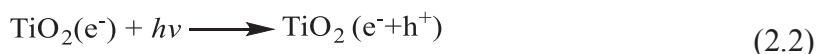
UV photocatalysis mechanism includes generation of the valence band (*VB*) to a source of holes (h^+) and conduction band (*CB*) produce electrons (e^-) when the energy of photon higher or equal to photocatalyst semiconductor band gap ($h\nu \geq E_g$). Water-splitting reaction is an endothermic reaction. It requires Gibbs Free Energy Change (ΔG^0) of 237 kJ/mol or 1.23 eV (X. Chen et al. 2010).



Photocatalytic water splitting reaction consists 4 steps:

- i) Electron(e⁻) – hole(h⁺) generation
- ii) Electron(e⁻) – hole(h⁺) trapping
- iii) Electron(e⁻) – hole(h⁺) recombination
- iv) Photocatalytic degradation (Chang et al. 2017).

i) Electron(e⁻) – hole(h⁺) generation; TiO₂ photocatalysts are irradiated with a wavelength of less than 385 nm, produce a strong oxidation ability. In this way, electron (e⁻) transfer is actualized from valence band to conduction band and occur energy gap called holes (h⁺) in the valence band. In this way, electron (e⁻) and hole (h⁺) pairs are produced (Hodd 1979).



The holes assist the oxidation reaction of organic compounds via the formation of hydroxyl radicals, the electrons assist reduction and oxidation reaction with together via the formation of superoxide radicals.

ii) Electron(e⁻) – hole(h⁺) trapping; (e-h +) pairs are captured by electron and hole scavengers and inhibits recombination. Electrons are attracted by acceptors; photo-irradiated holes react with electron donors in the adsorbed species with different phase.

A photocatalyst is qualified by the ability to absorb reduced and oxidized reactants at the same time. Furthermore, semiconductor's band gap position and the adsorbate redox potential are managed to transfer the electron from the conduction band to the adsorbed particles (acceptor). When adsorbate is a donor, valence band position should be below to donate an electron valence band empty holes. Electron transfer from semiconductor to adsorbate is a reduction mechanism, the opposite site is termed oxidation mechanism (Indian Institute of Science (Bangalore) and Madras 1914).

The reduction is determined by conduction band electrons energy levels; oxidation is determined by valence band holes. Adsorbed couples water (H₂O) and oxygen (O₂) are oxidized by holes and separate into OH and H⁺. Oxygen reduction produces superoxide radical anions (·O₂⁻) by an electron in the conduction band. These radicals react with H⁺ and produce hydrogen dioxide radical (·HO₂, hydroperoxyl) and

collide with electron to produce hydrogen peroxide (H₂O₂) (Indian Institute of Science (Bangalore) and Madras 1914).

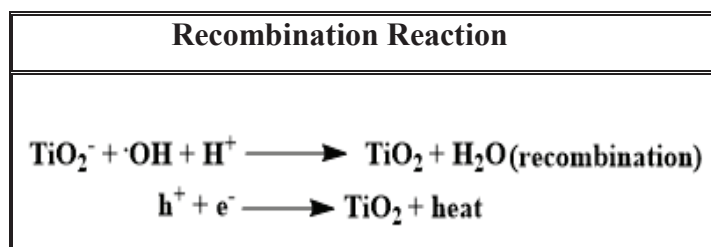
This photocatalytic process includes reactive oxygen species (ROS) and hydroxyl radicals (\cdot OH) are listed below:

Table 2.2. Reactive species reactions in photocatalysis

Reactions of the Ejected Electrons from the Conduction Band
$\text{TiO}_2(e^-) + \text{O}_2 \longrightarrow \text{TiO}_2 + \cdot\text{O}_2^-$
$\text{TiO}_2(e^-) + \cdot\text{O}_2^- + 2\text{H}^+ \longrightarrow \text{TiO}_2 + \text{H}_2\text{O}_2$
$\text{TiO}_2(e^-) + \text{H}_2\text{O}_2 \longrightarrow \text{TiO}_2 + \cdot\text{OH} + \text{OH}^-$
$\cdot\text{O}_2^- + \text{H}_2\text{O}_2 \longrightarrow \cdot\text{OH} + \text{OH}^- + \text{O}_2$
$\cdot\text{O}_2^- + \text{H} \longrightarrow \cdot\text{HO}_2$
$\text{TiO}_2(e^-) + \cdot\text{HO}_2 \longrightarrow \text{TiO}_2 + \text{HO}_2^-$
$\text{HO}_2^- + \text{H}^+ \longrightarrow \text{H}_2\text{O}_2$
$2\cdot\text{HO}_2 \longrightarrow \text{O}_2 + \text{H}_2\text{O}_2$
Reactions of the Holes in Valence Band
$\text{TiO}_2(h^+) + \text{H}_2\text{O} \longrightarrow \text{TiO}_2 + \cdot\text{OH} + \text{OH}^+$
$\text{TiO}_2(h^+) + 2\text{H}_2\text{O} \longrightarrow \text{TiO}_2 + 2\text{H}^+ + \text{H}_2\text{O}_2$
$\text{TiO}_2(h^+) + \text{HO}^- \longrightarrow \text{TiO}_2 + \cdot\text{HO}$

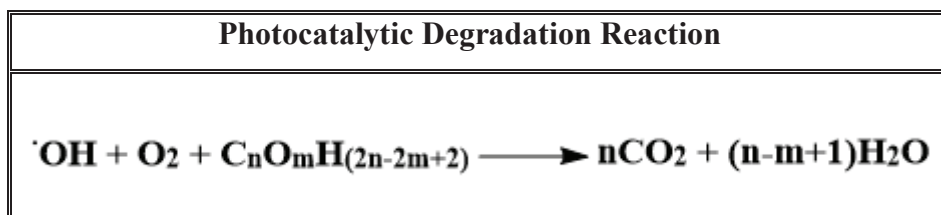
iii) Electron (e⁻)-hole(h⁺) recombination; electrons and holes contest to each other and deactivation of charge carrier can be occurring in the surface or bulk of the photocatalyst. There is a coincidence that electron (e⁻) and hole (h⁺) recombination to charge transfer to adsorbed compounds in contestation with occurred picoseconds(ps) or nanoseconds(ns). Charge-pairs (e⁻ - h⁺) are formed very fast in femtosecond (fs). Electrons (e-) and holes (h+) are trapped in approximately 10 nanosecond (ns). The characteristic time of recombination interval is 10 ns to 100 ns. Recombination is occurred by the photocatalyst semiconductor surface with release heat. Recombination reaction process is shown in Table 2.3 (Gnaser, Huber, and Ziegler 2004).

Table 2.3. Recombination reaction at TiO₂ photocatalysis



iv) Photocatalytic degradation; Photo-irradiated e⁻ and h⁺ oxidize and react adsorbed compounds on the surface and generate (·OH) radicals. Strong oxidizing agent as a (·OH) radicals reacts with any volatile organic compounds (VOC) with hydrogen bonding and electrostatic interaction. (·OH) radicals have the highest electron density and choose carbon atoms to produce harmful organic chemicals into carbon dioxide and water (Mo et al. 2009).

Table 2.4. Photocatalytic degradation reaction with any volatile organic compounds



Briefly, the superoxide anions (·O₂⁻) and hydroxyl radicals (·OH) have strong oxidizing ability. They choose the carbon atom to become reaction with organic compounds by power of redox reaction.

There are some factors to affect photocatalytic activity process such as calcination temperatures, light intensity, particle size, pH, surface area, oxygen pressure, catalyst loading and crystallinity are important factors to affect photodegradation efficiency. When different type of TiO₂ materials are considered, anatase phase TiO₂ is preferred for activation of electrons to used self-cleaning materials. An illustrated representation of TiO₂ photocatalysis mechanism is shown in Figure 2.5. (Li and Li 2017).

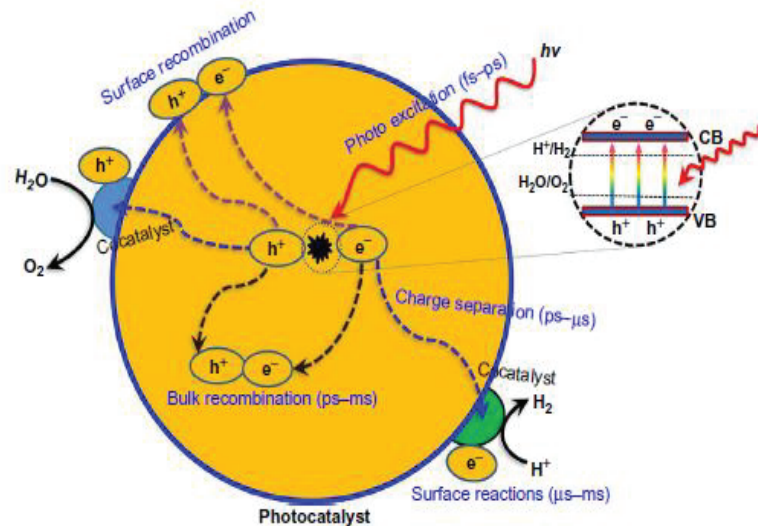


Figure 2.5. Photocatalytic water splitting mechanism (Source: Li and Li 2017).

2.5. Cleaning Methods of Solar Panels

One of the most important problem is the pollution of airborne dust on the panel surface is caused by reducing solar energy electrical output (Kasim, Al-Wattar, and Abbas 2010). For long term operation of the solar panels, it will be necessary to develop new techniques to remove the dust accumulated on the surface without losing the efficiency.

2.5.1. Natural Methods

It is used to remove dust such as natural powers, rainwater, wind energy and gravity. The solar cell array should turn vertical or necessary position to get rid of contamination when every weather condition of seasonal. However, the rotation of the huge solar cell array is very inconvenient. Therefore, this method is not controllable due to changes in climate conditions (Darwish et al. 2013).

2.5.2. Mechanical Methods

It is based on cleaning the solar panel surface by brushing, blowing, vibrating devices or ultrasonic methods. The very small size of the dust is very strong to adhere to the solar panel array with the influence of Van der Walls forces. The cleaning forces must overcome these intermolecular attractions (Darwish et al. 2013).

The brushing methods are inefficient due to the adhesion of small size pollutions to the surface. Also, considering the places where solar panels are installed, the cleaning machines are difficult to maintain and transport. In addition, the solar panel surface may be damaged during wiping. The wind blowing method is not an effective method because of its low efficiency and high energy consumption (Kaldellis, Fragos, and Kapsali 2011). The vibratory and ultrasonic removal of dust has also been recently introduced and is not available due to the fact that the studies have already begun (Kaldellis and Kokala 2010).

2.5.3. Electrostatic Methods

In this method, a transparent electrodynamic layer is designed to protect the panels from an accumulation of dust. This layer includes a transparent panel with embedded parallel electrodes connected to a single-phase (AC) source to generate an electromagnetic wave (Sims et al. 2000).

The electromagnetic field generated by the electrodes on the surface of the panel pushes the dust particles accumulated on the panel surface and prevents the accumulation of other particles if charged by positive or negative polarization. If the particles are not charged, they will be temporarily deposited on the panel surface, but will then be exposed to a non-homogeneous electric field. This movement of particles causes electrical charges and electromagnetic fields then removes them from the surface (AbdulHussain et al. 2016).

2.5.4. Self-Cleaning Methods

All previous methods try to remove the dust from the outer layers from the photovoltaic cells but, volatile organic compounds (VOCs) make non-covalent bonds with the surface of the cells and it is very difficult to remove the dust from outer layers by conventional methods.

2.5.4.1. Volatile Organic Compounds (VOCs)

Volatile organic compounds can be regarded as any organic compound (VOC) is excess from (0.1 mmHg) vapor pressure under standard conditions (25 °C and 760 mmHg) (Centi and Perathoner 2014). They are usually found in industrial wastes as by products or unused reagents, and their emissions have prevalent environmental impacts.

These volatile organic compounds have low molecular weight, high vapor pressure and hydrophobic structure (Štangar et al. 2015).

Volatility is mainly due to intermolecular forces such as the forces of Van der Waals interaction in these compounds. (VOCs) are usually present in the form of gases like CH₄ or liquids as CH₃OH and rarely solids like naphthalene (Mo et al. 2009). Because of their volatility, they contaminate air, water and soil and they move from one place to another very easily by air (Faisal I. Khan and Ghoshal 2000). Industrial types of volatile organic compounds are shown in Table 2.5.

Table 2.5. Volatile Organic Compounds (VOC) and Types (Source: Herrmann 1999).

Name	Sources
Alkanes (CH ₄ , etc..)	Fuels, solvent, vegetation, animal wastes
Alkenes (C ₂ H ₄ , C ₄ H ₈ , etc..)	Engine exhaust, foundry operations, petroleum refineries, plants
Aryl hydrocarbons (benzene, naphthalene, etc..)	Gasoline, tobacco smoke
Aldehydes, ketones (acetaldehyde, acetone, etc..)	Industries, incinerator emissions, spray painting, polymer manufacture, petrochemicals
Alcohols (methanol, ethanol, etc..)	Industries, solvents, antifreeze, additives of gasoline
Epoxides (ethylene oxide)	Industries (monomer for synthesis of polymers)
Carboxylic acids and phenols (acetic acid, phenol, etc..)	Baking industries, latrines, toilets, phenolic soaps
Ethers (Diethyl ether)	Anaesthetics, additive to gasoline
Halogenated hydrocarbons (vinyl chloride, freons)	Leakage from refrigerator, dry cleaning solvent, etchant, plasma reactors
Nitrogen containing organic compounds (amines, nitro compounds)	Antioxidants, curing agents in plastics manufacture, drugs, pesticides, dyes, pigments, inks

Since a large number of harmful volatile organic compounds (VOCs) can be oxidized by hydroxyl radicals, chemical oxidation processes can be considered as a possible alternative method of cleaning of air, water and surface pollutant control (Lisi 2002). It is a promising method for the destruction of toxic and bio-resistant organics and some inorganic substances. It can be used to obtain transparent self-cleaning coatings on various surfaces such as solar panels that do not any limiting cleaning and maintenance

operations, thereby reducing costs and improving the quality of the cleaning surfaces and the efficiency of sunlight (Nishimoto and Bhushan 2013).

Because of its photo-activated properties provides the self-cleaning (TiO_2) surface by sunlight, it becomes hydrophilic and thus forms a homogenous water film that prevents contact between the outer dust and the substrate itself and enables photo-separation of contaminants. The formation of a water film to degrade of pollutants on surfaces can cause a real self-cleaning effect. (Yao and He 2014). Under UV illumination, the surface of TiO_2 becomes hydrophilic with a water contact angle close to 0° , and the surface is easily cleaned with water. This effect will be discussed in detail in the following sections (Yao and He 2014). TiO_2 -coated substrates can achieve excellent self-cleaning property when exposed outdoors as shown in Figure 2.6.

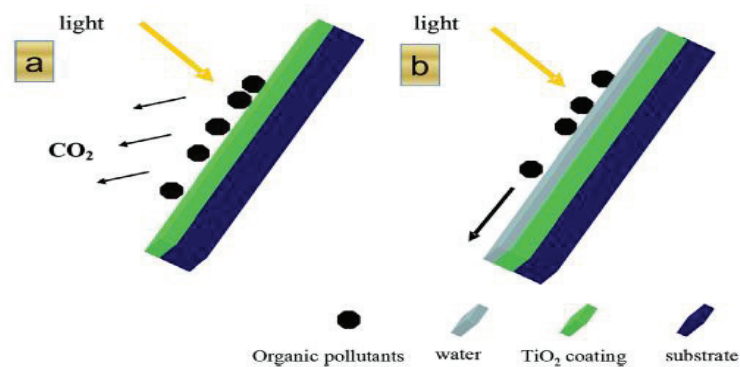


Figure 2.6. a) Photocatalytic degradation of organic pollutions b) Removal of pollutions by water due to the hydrophilicity of TiO_2 surface (Source: Yao and He 2014).

2.6. Applications of TiO_2 Photocatalyst

Due to the high chemical activity of photocatalysts, numerous studies have been carried out on environmental applications. These photocatalysts can be used in the removal of organic impurities in the air and water, as well as in many areas from water to hydrogen ions (Stathatos, Petrova, and Lianos 2001).

There are many environmental application areas of TiO_2 in heterogeneous photocatalysis. TiO_2 have several advantages over other semiconductors which are photocatalytically active colorless so provide enter the sunlight to absorbing surface

easily, low cost, non-toxic, thermally stable, inert versus acids and solvents, highly photoactive, can be recycled and self-regenerating.

Titanium dioxide (TiO_2) photocatalysis applications are shown in Figure 2.7. These applications are classified anti-fogging effect, water purifier effect, air-cleaning effect self-cleaning effect and anti-bacterial effect (Gamage and Zhang 2010).

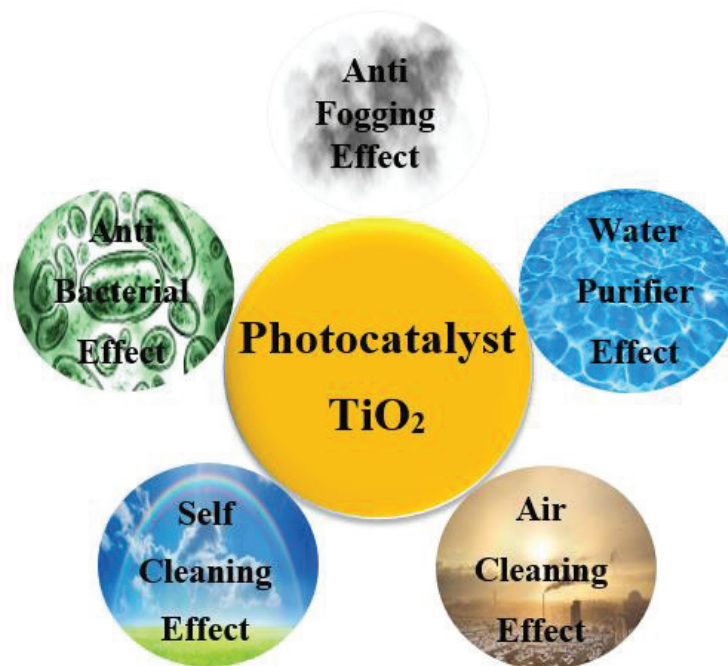


Figure 2.7. Photocatalyst Applications

2.6.1. Anti-Fogging Effect

One of the major applications of TiO_2 photocatalyst is anti-fogging effect. When the steam cools down on mirror and windows surfaces to form lots of water droplets fogging of the surfaces occurs. As is known, existing solutions have many disadvantages Anti-fogging sprays do not rely on washing and it must be reapplied regularly. Permanent coatings increase wettability and surface energy, this high surface energy is also prone to surface pollution. Owing to TiO_2 anti fogging properties, there is no water droplets occurs on a highly hydrophilic surface. Uniform water thin film is formed on the highly hydrophilic surface. This hydrophilic water thin film prevents fogging. When the surface is very hydrophilic, it shows anti-fogging properties for a few days or a week. That's why it can be decrease the costs connected to environmental pollution problems (Hashimoto, Irie, and Fujishima 2005). Anti-fogging coatings are very interesting for many

applications, like solar cell that improves absorbance efficiency, windshields that can keep high visibility and provide safe driving, also it can be applied organic ophthalmic lenses that prevent loss of performance (Chemin et al. 2018).

2.6.2. Water Purifier Effect

Photocatalysis has been used to remove polluted groundwater using parabolic solar condensate type reactors. Because of its ability to mineralize many organic contaminants. It has been used at the scale of engineering for the solar photocatalytic treatment of persistent chlorinated water pollutants in the industry and the treatment of wastewater from a resin plant. This process has also been shown to be effective in the treatment of wastewater from a 5-fluororacyl (cancer drug) production plant, pulp and paper mill wastewater treatment, dye house wastewater and oil field.

Furthermore, titania photocatalysis has been shown to be effective in removing microbiological pathogens and chemical compounds from water. The effect of the disinfection of TiO₂ suspensions of photocatalysis applications are used extraction of biological species. The effect of additives and pH, the photocatalytic abilities of TiO₂ thin films and the effect on the disinfection and the electrochemically applied effect potential on the photobactericidal effect of TiO₂ thin films for drinking water disinfection (Gamage and Zhang 2010).

2.6.3. Air Cleaning Effect

In modern society, people often complain about the horrible indoor air quality. Indoor air pollutants have complex compositions. Most pollutants have low concentrations like sub-ppm or ppb. The TiO₂ photocatalytic process is considered to be an effective technique for photodegradation of air pollutants (Beeldens 2006). Because it can break down many types of air pollutants. Air purifying photocatalytic materials are also used in the control of external air pollution. The light irradiation intensity is higher than in the interior in the outdoor environment, so air cleaning photocatalytic materials performs better outdoors (Benedix et al. 2000). The system of photocatalyst TiO₂ also perform a permanent and automatic deterioration of air pollutants due to direct contact between the ambient air and the surfaces of the photocatalyst. Therefore, photocatalytic materials of TiO₂ are efficient and economically suitable candidates for air purification (Guo, Wu, and Zhao 2009).

2.6.4. Self-Cleaning Effect

Owing to photocatalytic activity of TiO_2 surface exhibits excellent self-cleaning properties with super-hydrophilicity; therefore, it has already been used in various industrial products like glasses, fiber, screen doors, verandas, bathrooms, plastic films and tent materials (Beeldens 2006).

Adsorbed pollutions on TiO_2 surface can easily cleaned because water enters the pollution and high hydrophilic (TiO_2). Volatile organic composites can be destroyed via TiO_2 photocatalyst to form a clean surface. Also, TiO_2 coated surface like windows can protect transmission properties and have high refractive index that's why it enhances the reflection of light (Lisi 2002). Figure 2.8. compared with solar panels without self-cleaning coating films and solar panel with self-cleaning coating films.

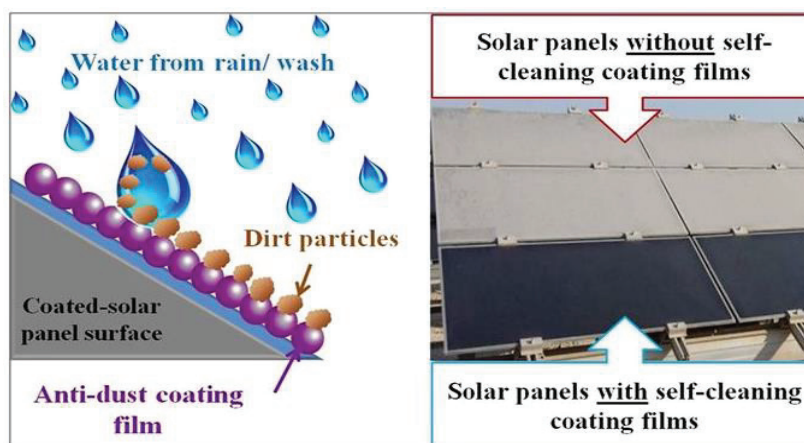


Figure 2.8. Schematic representation of self-cleaning coated surface
(Source: Isaifan et al. 2017).

2.6.5. Anti-Bacterial Effect

There are lots of work inactivation of bacteria, viruses, molds and cancer cells to using immobilized TiO_2 photocatalyst (Kikuchi et al. 1997). This photo catalyst is not only killing bacterial cells but also helps in breaking down the cell itself. Studies have shown that the titanium dioxide photocatalyst is more effective than other antibacterial agents because the photocatalytic reaction works when the surface is covering active cells and the bacteria continue to proliferate (Chan et al. 2013). Titanium dioxide has a long-lasting antibacterial effect due to its reactive structure (Akhavan 2009). Briefly, cells

exposed to TiO₂ photocatalysis show rapid cell inactivation in regulatory and signaling, a strong reduction in coenzyme independent respiratory chains, reduced iron and phosphorus to lower levels in assimilation and transport, a lower capacity for biosynthesis and both (Fe-S cluster) destruction of groups (Kubacka et al. 2014). Figure 2.9. shows number of living bacteria on TiO₂ thin films after irradiated of 30 min interval.

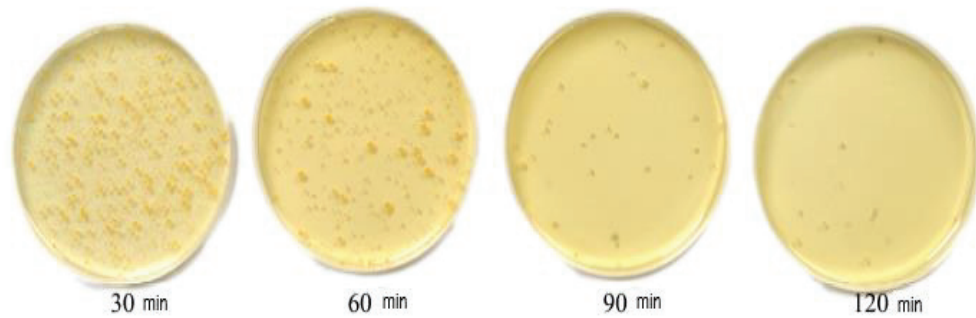


Figure 2.9. Number of living bacteria on TiO₂ thin films after irradiation of 30 min interval (Source: Efendiler et al. 2014).

Besides, nanoscale TiO₂ semiconductors have great importance in the destruction of pesticides in agriculture field determine of their residues and protection of agricultural crops (Wang et al. 2016). As shown in the above specifications, titanium dioxide (TiO₂), the unique semiconductor photocatalytic properties of air and water purifier, food, cosmetics, ceramic and construction industry as an additive, mildew and bad deodorizing agent, as well as photocatalytic device and high temperature gas sensors, anode in lithium batteries as a biosensor or biocompatible material in bone implants, it is also widely used in a variety of applications such as optoelectronic devices and solar cells (Ohno et al. 1999).

2.7. Importance of Hydrophilicity

Contact angle (θ) is a measurement of the angle formed between the solid surface and line tangent of a particular droplet radius of the contact point on a solid. The contact angle is linked to surface tension by using Young's equation. This depends on certain solid-liquid interaction. The 0° contact angle causes the surface to wet, while an angle between 0° and 90° causes the drop to spread slightly due to the molecular

attraction. Angles greater than 90° indicate that the liquid tends to be bead or shrinkage on the solid surface (Lisi 2002). 2D representation of hydrophilic, hydrophobic and superhydrophobic surface are illustrated in Figure 2.10.

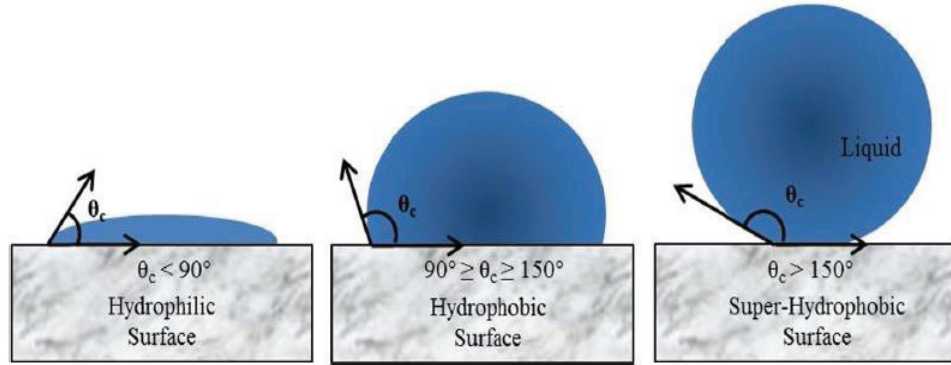


Figure 2.10. Contact angles according to material surface (Source: Gomes, De Souza, and Silva 2013).

There is a relationship between the contact angle and the surface tension. (Young's Equation).

$$\gamma_s = \gamma_{sl} + \gamma_l \cdot \cos\theta \quad (2.3)$$

(γ_s) and (γ_{sl}) are surface free energies per unit area (surface tension) of the solid and liquid orderly. Their units are (J/m^2) or (N/m) .

According to Girifalco and Good, equation is shown is below as;

$$\gamma_{sl} = \gamma_s + \gamma_l - 2\phi(\gamma_s \gamma_l)^{1/2} \quad (2.4)$$

In this equation, ϕ is a constant parameter. These two equations are combined and contact angle is simply shown as;

$$\cos\theta' = r\cos\theta \quad (2.5)$$

(θ') is a contact angle and (r) is a surface roughness ratio between actual and apparent surface area. This equation shows that the surface roughness increases the hydrophilicity of hydrophilic surfaces ($\theta < 90^\circ$) and also increases the hydrophobicity of hydrophobic surfaces ($\theta > 90^\circ$) (C. C. Chen et al. 2008).

Water-affinity materials are called hydrophilic which can easily absorb water. According to surface chemistry, such materials get wet to form a layer of the water film. In addition, the hydrophilic materials have high surface tension and are capable of forming "hydrogen bonds" with water. After UV illumination, TiO₂ gains hydrophilic properties. The photo-irradiated hydrophilic material comprises electron reduction of Ti (IV) cations to Ti (III) and forms holes in the lattice regions or above the semiconductor surface. This kind of trapped holes are weakened to bonds between the relevant titanium and the lattice oxygen causes loosening of the oxygen atoms, thus generate oxygen vacancies. The photo-irradiated holes used up bulk of TiO₂ which spread on the surface and the lattice oxygen regions. Most of the trapped holes are used up to directly react with adsorbed organics or to produce water-adsorbed ($\cdot\text{OH}$) radicals. However, it reacts with a small portion trapped holes of TiO₂ in the titanium region, and break down between the lattice titanium and oxygen ions which coordinated water molecules at titanium region.

The coordinated H₂O molecules leave off a proton and then a new (OH) group has consisted and this leads to an increase in the number of (OH) groups on the surface. Single coordinated thermodynamically less stable new (OH) groups produced when irradiating of UV light than double coordinated (OH) groups.

For this reason, the TiO₂ surface covered less stable (OH) group than initial (OH) group thermodynamically. Lots of chemical absorbed (OH) leads to an increase in the forces of hydrogen bonding and Van der Waals interactions among H₂O and OH in the medium. Water can easily cover throughout the surface and the hydrophilic properties will increase as illustrated in Figure 2.11 (Carp, Huisman, and Reller 2004).

The hydrophilic regions are aligned along the bridge oxygen regions. Reduced regions can be re-oxidized with air and weakly bound hydroxyl groups desorb from a more hydrophobic form. The photo-irradiated hydrophilic process is always gently inverted in the dark because the contaminants are slowly absorbed on the surface, thus returning it more hydrophobic form. The oxygen in the air is responsible for the oxidation of the hydrophilic surface from (Ti⁺³) to (Ti⁺⁴) states throughout the dark (Vernardou et al. 2009).

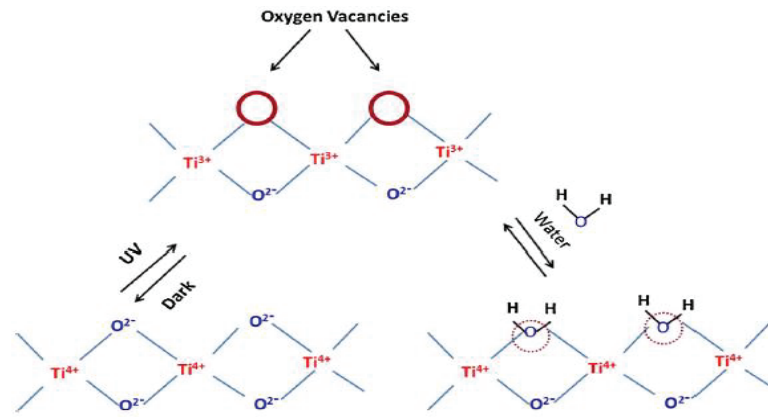


Figure 2.11. Schematic representation of photoirradiated hydrophilicity. Vacancies will provide hydrophilic surface to increase the affinity to water molecules (Source: Banerjee and Pillai 2015).

The effect of self-cleaning with photocatalysis and hydrophilicity is maintained. Due to the hydrophilic properties of the surface, the chemically bonded water layer formed on the thin film is adsorbed to the surface with the effect of van der Waals and hydrogen bonds. This process is shown in Figure 2.12. In this way, pollutants can easily be removed by water spreading to the surface. That's why the surface gains self-cleaning properties (Schneider et al. 2012).

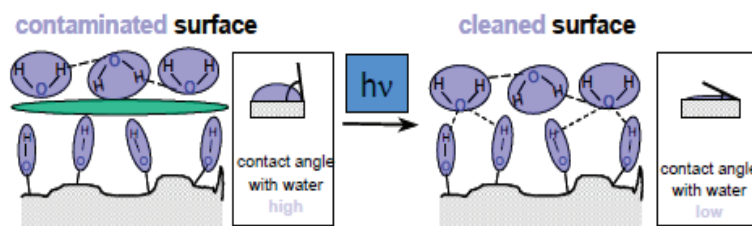


Figure 2.12. The process of self-cleaning of TiO_2 surface with photocatalytic effect (Source: Schneider et al. 2012).

2.8. Band Gap Theory of TiO_2

The band gap of semiconductors causes resonance absorption at least one of the light having a wavelength λ_{bg} corresponding to least E_{bg} . There are two main band gap transition types in semiconductor as direct band gap transition and indirect band gap

transition. These two types of band gap transition depend on the crystal structure of the semiconductor (Tang et al. 1994).

There is electrically dipole permission to pass from valence band to conduction band indirect bandgap transition. If wave factor k value is 0, the direct transition is forbidden but, k value is not equal to 0, the direct transition is allowed in some material.

At indirect bandgap transition, passing from valence band to conduction band is electrically dipole forbidden. The transition has occurred with the help of phonons. Both energy and momentum of the pair of electrons and holes are changed in transition. When compared to direct transition, absorption and emission of light are lower because of momentum change (Serpone, Lawless, and Khairutdinov 2005).

The band gap energy of TiO_2 on the optical transmission can be obtained by using the Tauc law equation (Tauc and Menth 1972):

$$(\alpha h\nu)^n = \mathcal{A}(h\nu - E_g) \quad (2.6)$$

Where E_g is an absorption band gap energy, α is a Titania absorption coefficient, $h\nu$ photon energy (*in Ev*), \mathcal{A} is a absorption constant and n is an optical transmission mode (Tiefeng et al. 2009).

The anatase phase of TiO_2 is accepted as an indirect band gap semiconductor. That's why band gap energy (E_g) has been obtained for the indirect transition that can be attained the intersection of the extrapolated linear part of the $(h\nu)$ versus $(\alpha h\nu)^2$ curve (Koseoglu et al. 2015).

There are some controversies about the nature of the band gap transition in anatase thin films. There is not enough information about the nature of the single crystal anatase band gap transition. G. Cangiani et. al. calculated that direct minimal band gap energy of rutile 1.86 eV and indirect band gap energy 1.89 eV (G. Cangiani, 2003). N. Daude working group and H. Mathieu group investigate that 3.034 eV and 3.049 eV at 1.6 K are found direct and indirect values of band gap transition in rutile (H. Mathieu, 1978), (Daude, Gout, and Jouanin 1977).

It is claimed that the absolute values for band gap energies cannot be obtained because of the nature of the band gap energy calculations. However, there is a little difference in bandgap energies between different transitions. G. Cangiani et. al. were

investigated that minimum band gap energy of anatase was 2.11 eV, band gap transition was occurred indirectly.

Direct band gap transition was calculated as 2.57 eV for anatase. Single crystal anatase band gap energy value was calculated 3.2 eV in experimental results by D. Dumitriu group (Dumitriu et al. 2000). There are not any reports for the nature of the bandgap transition in anatase. There are very few structural differences between anatase and rutile but their electronic properties are similar (H. Berger, Tang, and Lévy 1993).

2.9. Enhancement of Photocatalytic Activity of TiO₂ Thin Films

Many methods have been accepted to increase the photocatalytic efficiency of TiO₂. These can be summarized as chemical changes, such as the addition of some components to the TiO₂ for structural changes, increasing surface area and porosity (X. Chen and Mao 2007).

There is a reason for doping (TiO₂) to improve photocatalytic activity. Doping increase the number of photons and quantum efficiency of catalyzed redox reaction potential. This can be done by extending the lifetime of the pairs of electrons and holes (charge carriers) separated by stimulating the shallow (trapping) site. The energy levels of the shallow site do not very deep in the band gap. If the electrons and holes are too firmly attached to the shallow zone, they can not relocate to the surface and cannot attend in the redox reaction and recombination takes place. Shallow zone permits to enhance of a lifetime when electrons and holes are active for redox reaction and increase localized levels between the band gap so, the semiconductor is able to absorb supra-light and become more efficient (Panayotov and Morris 2009).

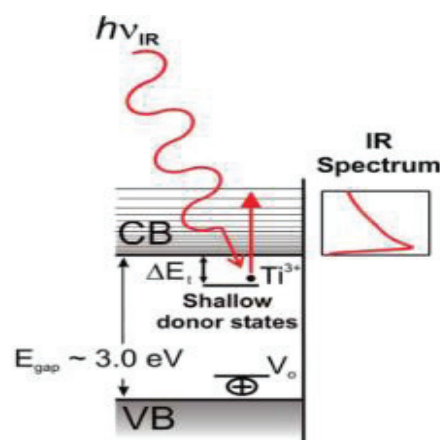


Figure 2.13. When semiconductor excite with IR radiation, electrons are trapped in shallow state (Panayotov and Morris 2009).

Also, doping reduce the band gap energy, allow the optical absorption line to shift to the red side. This increases the photocatalytic activity under visible light illumination. This makes it possible to eliminate the requirement of using a UV lamp in sunlight. The use of doping materials may provide an increase in electrical conductivity and repair other defects (T. Berger et al. 2005).

2.9.1. Ruthenium (Ru) doped TiO₂ Thin Film

Among all transition metal dopants, ruthenium (Ru⁺) has very effective for the increment of TiO₂ photocatalysis. When Ruthenium doped TiO₂, impurity energy level has occurred. Ru⁺ fermi level lower than undoped TiO₂ fermi level and photo-induced electrons easily transferred from conduction band (CB) to doping material of Ru⁺ impurity level. Ru⁺ ions increase photo-induced electron-hole pairs and widen absorption from ultraviolet (UV) to visible light to form intermediate energy level. (Ohno et al. 1999). Ru⁺ doping TiO₂ increases electron conductivity and decreases recombination possibility of charge carrier. The electrons deposited on the ruthenium metal particles can be transferred to protons which are adsorbed on the surface and these protons are reduced to hydrogen molecules. Therefore, ruthenium metal particles with suitable work functions have a high photocatalytic activity which can assist in electron transfer (Hamzah et al. 2012). Low-proportion of Ru⁺ doping increases the photo-electrochemical water splitting on TiO₂ surface (Luo et al. 2016). If a large amount of Ru⁺ doped in TiO₂, photocatalytic activity is lowered by recombination center is formed (Ohno et al. 1999).

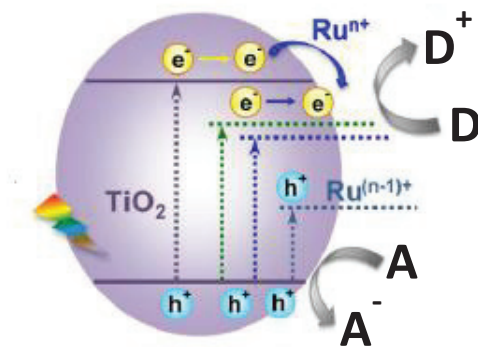


Figure 2.14. Schematic illustration of energy level Ruthenium (Ru⁺) metal doped TiO₂ (Source: Luo, S. et al. 2016).

Ru^+ impurity level prevents electron-hole recombination. Studies have shown that Ru^+ doped photocatalyst has wavelengths of visible light longer than 440 nm as an electron acceptor. Also, it provides to reduce band gap energy and cause anatase to rutile transformation at low temperatures. Ruthenium can increase visible light absorption through surface plasmon resonance of ruthenium nanoparticles. Ruthenium has ability to decrease recombination to trapping excited electrons throughout the entrance of fermi level of ruthenium. Fermi level of Ru^+ is located just below the TiO_2 conduction band, and therefore the TiO_2 electrons doped with ruthenium can be able to tunnel through the potential barrier as shown in the Figure 2.14 (Bakardjieva and Murafa 2009).

Also, Ru^+ doping increase in photodegradation efficiency (Senthilnathan et al. 2010). Doping of ruthenium causes a decrease anatase grain size and that's why the surface area of the samples increases. Growing crystal defects of anatase grain behave as nucleation sites for crystal conversion and enhance to the surface of the Ru^+ particles (Gu et al. 2013).

CHAPTER 3

EXPERIMENTAL PROCEDURE

3.1. Growth of Ruthenium (Ru⁺) Doped TiO₂ Thin Film

In this study 1 mm soda lime glass slides were used as a substrate to grow Ruthenium (Ru⁺) doped Titanium dioxide (TiO₂) films on it. They were cleaned in an ultrasonic bath with acetone, methanol and pure water orderly. The substrate to target distance was kept at 7.3 cm for each deposition into growth chamber. When the system pressure reaches 100 mTorr, turbo pump is worked and pressure reaches the 10⁻⁶ Torr Ruthenium doped TiO₂ thin films will be formed using power and gas flow values optimized for Ti and Ru thin films. Heat will be applied at 500°C to obtain the anatase phase of TiO₂.

After reached chamber pressure, 36 sccm Ar⁺, 4 sccm O₂ gases was send into the sputter chamber due to mass flow controller and applied D.C. power for Titanium (Ti) target and 86 sccm Ar⁺ and 4 sccm O₂ gases sent into the chamber for Ruthenium (Ru⁺) target was used. When the DC power supply is running and Argon gases were ionized that cause to break over the target atoms to accumulate on the substrate.

There are little magnets located under the target part to redirected plasma and increment collision. When target uploaded negatively, argon ions accelerated through the target gives their energy to the Ti and Ru targets and stick the surface of the glass substrate. The sample holder was rotated in order to access homogenous surface during deposition. Valve position was changed to get optimum pressure.

150 Watt DC power for Ti and 40 Watt for Ru target is applied to generate plasma. Before started deposition, 5 minutes pre-sputtering was performed to each thin film growing to get rid of any contamination of the target's surface. That's why shutter is used between target and substrate throughout pre-sputtering. All growth parameters are listed in Table 3.1. and the schematic representation of the growth chamber is shown in Figure 3.1. and Figure 3.2 and uncoated SLG, undoped and Ru-doped TiO₂ are shown in Figure 3.3.



Figure 3.1. The schematic representation of D.C. Magnetron Sputtering System

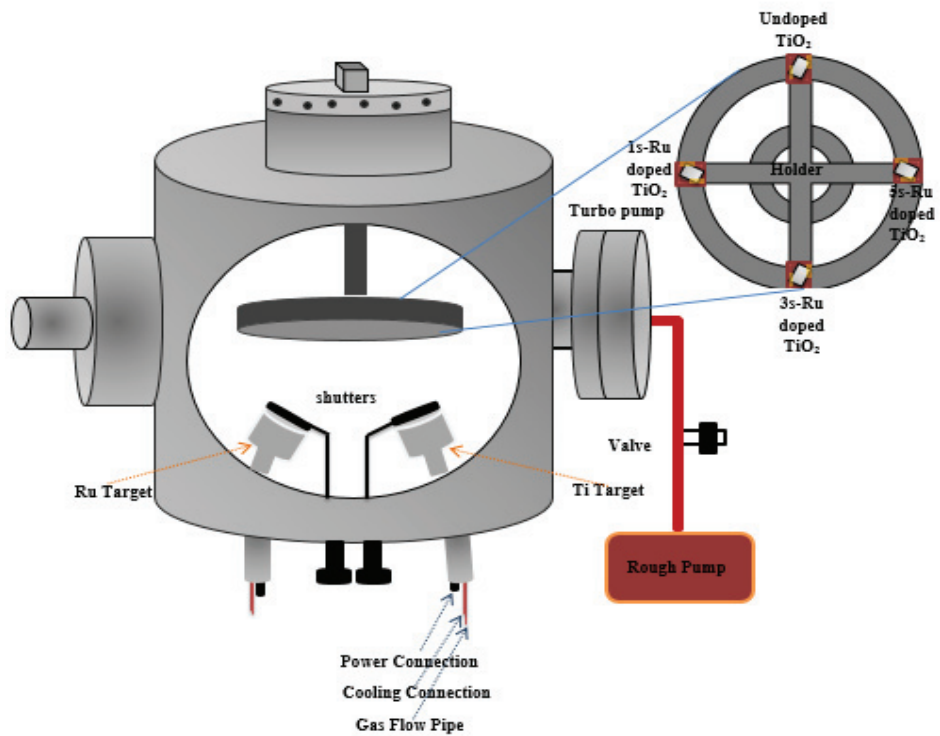


Figure 3.2. Representation of preparation thin film by a D.C. Magnetron Sputtering Technique

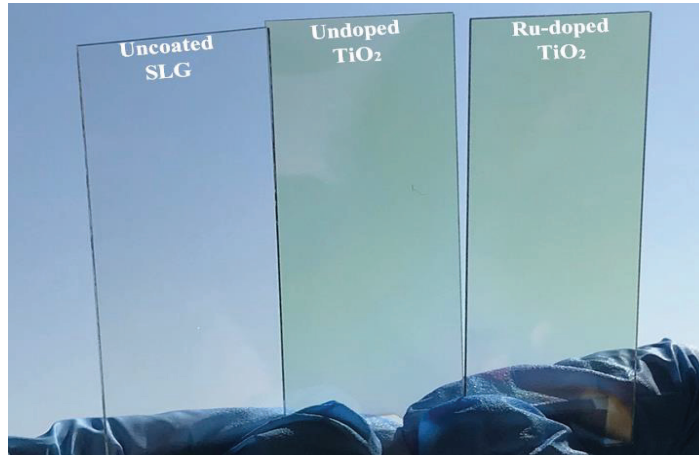


Figure 3.3. Images of Uncoated, Undoped and Ru-doped TiO₂ Thin Films

Table 3.1. Growth Parameters of Ru-doped TiO₂ thin Films for D.C. Magnetron Sputtering Technique

Sample	Deposition Time		Ar ⁺ gas (sccm)		O ₂ gas (sccm)		Power (Watt)		Thickness (nm)
	Ti (min.)	Ru (sec.)	Ti	Ru	Ti	Ru	Ti	Ru	Ru-doped TiO ₂ thin film
Undoped TiO ₂	15	0	36	86	4	4	150	40	38
1s-Ru doped TiO ₂	15	1	36	86	4	4	150	40	42
3s-Ru doped TiO ₂	15	3	36	86	4	4	150	40	45
5s-Ru doped TiO ₂	15	5	36	86	4	4	150	40	53
7s-Ru doped TiO ₂	15	7	36	86	4	4	150	40	54

3.2. Surface Characterization

After TiO₂ thin films were obtained, characterization of these films was started. Transmission of undoped and Ru-doped TiO₂ thin films were measured using an UV-vis-NIR spectroscopy measurement. The crystallization and crystalline transformations were measured by the X-ray diffraction device (XRD) in thin films. The surface morphology of thin films and EDX analysis was determined using scanning electron microscopy (SEM). To investigate the surface properties of films, scanning-tip microscopy (AFM) was used to obtain three-dimensional surface topography images at an atomic level.

3.3. Photocatalytic Degradation Test of Methylene Blue Dye

The photocatalytic activities of thin film photocatalysts were determined by the degradation of methylene blue (MB). Methylene blue degradation test is widely accepted in photocatalytic activity experiments. Methylene blue is a brightly colored cationic thiazine dye with molecular formula $C_{16}H_{18}N_3S^+Cl^-$ as shown Figure 3.4. Absorption maxima are 664, 614 and 292 nm as shown Figure 3.5.

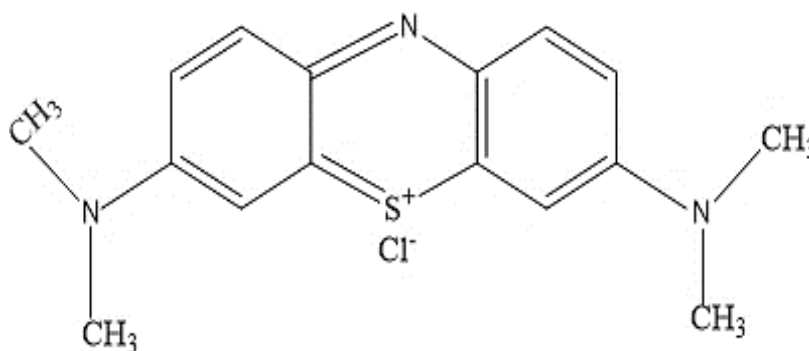
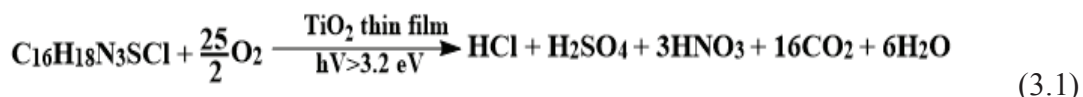


Figure 3.4. Chemical representation of Methylene Blue

In the photocatalytic activity experiments, a solution of methylene blue ($C_{16}H_{18}ClN_3S \cdot xH_2O$, at least 97% pure, Sigma Aldrich) prepared with de-ionized water (H_2O) was used as an organic impurity.

Before starting the experiments, aqueous solutions of methylene blue were prepared with known initial concentrations.

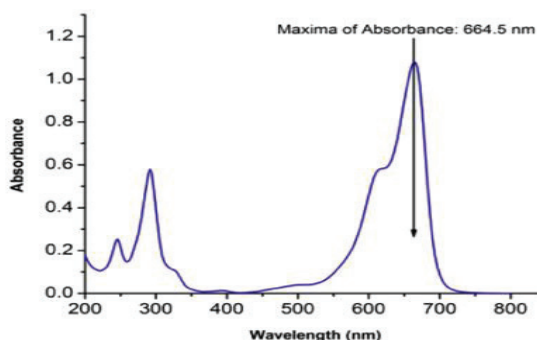


Figure 3.5. Absorbance spectrum of Methylene Blue under several wavelength stimulation (Source: Zou et al. 2016).

The absorption values of the prepared methylene blue solutions were evaluated with UV-Vis Spectrophotometer and calibration curve could be generated at a maximum wavelength of 664.5 nm. The concentration of methylene blue solution should be generated between the concentration ranges during the experiment. Photocatalytic degradation pathway of MB is shown Figure 3.6.

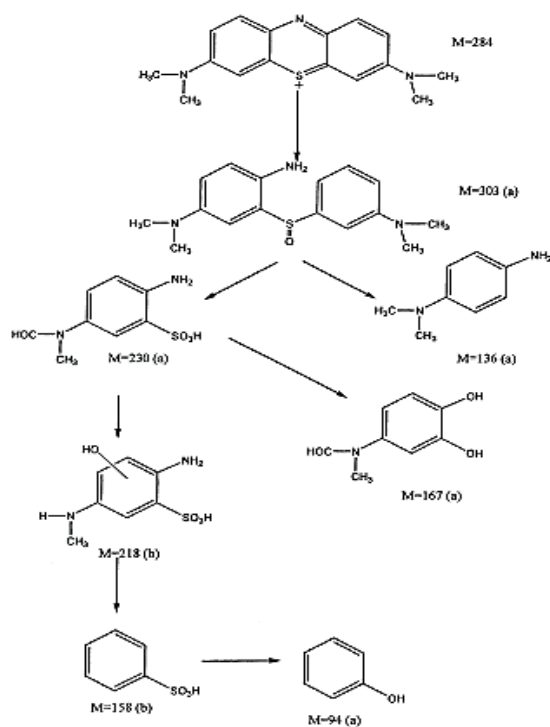


Figure 3.6. The photocatalytic degradation pathway of methylene blue using a) GC\MS and b) LC\MS (Source: Houas et al. 2001).

In this study, 15 ml and 1×10^{-5} M concentration of aqueous methylene blue solution was placed in the 50 ml beaker and Ru doped TiO_2 coated glasses (2 cm x 2 cm) were placed in solution. Approximately 2.5 ml of the solutions were taken and initial absorbance values were measured each prepared thin films with UV-Vis Spectrophotometer. (no doped, 1s-Ru doped, 3s-Ru doped, 5s-Ru doped, 7s-Ru doped). The initial concentrations could have calculated using the calibration curve the Beer-Lambert Law.

$$A = \epsilon \cdot l \cdot C \quad (3.2)$$

In the equation, the absorption coefficient ϵ of the liquid is expressed by the path l (10mm) and concentration C taken by the light in the liquid.

$$A = -\log\left(\frac{I}{I_0}\right) \quad (3.3)$$

For liquids, the absorption A , the intensity of the transmitted and incoming light are respectively I and I_0 . The absorption value of methylene blue at 664,5 nm is A . Relative concentration can be found when the A value can be measured.

$$\left(\frac{A_1}{A_0}\right) = \left(\frac{C_1}{C_0}\right) \quad (3.4)$$

Samples were placed and illuminated under the ultraviolet (Philips, TUV, 16 W) as in Figure 3.7. and there was 20 cm between the lamps and samples. All solutions were collected after illuminated under UV light with 2 hours intervals and the degradation methylene blue absorbance was measured by UV-Vis Spectrophotometer. The samples were emptied in the beakers again and the experiments were continued.

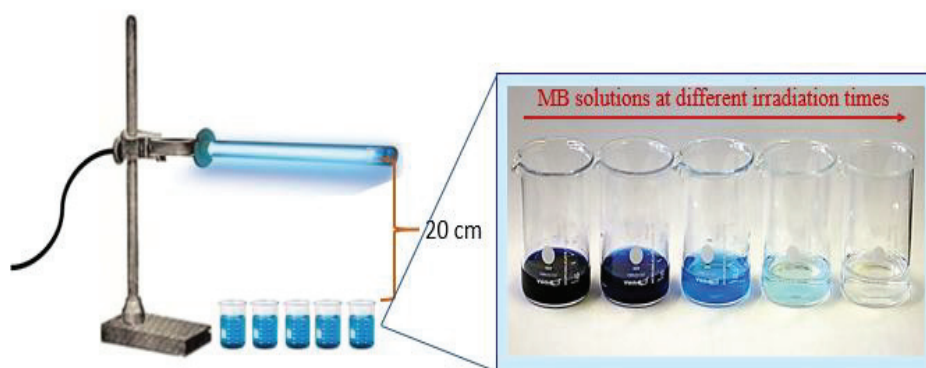


Figure 3.7. Schematic illustration of photocatalytic activity test experiment with methylene blue solutions

The degradation of methylene blue exposed photooxidation under ultraviolet light, it undergoes photo-sensitization and/or photo-oxidation depending on the type of catalyst under visible light. TiO_2 degradation of methylene blue under ultraviolet light; photolysis of methylene blue with the effect of ultraviolet light and it is expressed by

photooxidation by TiO₂. On the other hand, in visible light, methylene blue becomes sensitive to the reaction and injects electrons into the TiO₂ valence band.

Methylene blue degradation occurs only with the reaction in the equation for the inactive catalysts in visible light, but with the reactions in the equation for active photocatalysts in visible light. The reaction equations from 3.5 to 3.9 depend on the absorption behavior of methylene blue by the photocatalyst.



The degradation reaction of methylene blue at low concentrations (several ppm) complies with the 1st degree speed law.

$$\ln\left(\frac{C_0}{C}\right) = k \cdot t \quad (3.9)$$

C, C₀, k and t are methylene blue concentration, methylene blue initial concentration, rate constant and time respectively. Speed constants were determined by using concentration changes calculated as a result of photocatalytic activity tests.

3.4. Optical Characterization

In this study, spectrophotometer (PerkinElmer Lambda 950 UV/Vis/NIR) spectrophotometer with adjustable spectral bandwidth was used to measure the wavelength range of 200-2600 nm. Optical absorption and permeability of thin films were investigated at room temperature in the wavelength range of 250-700 nm.

3.5. Phase Characterization

Phase analysis (crystal structure) of the produced thin films samples was performed by X-ray diffraction (XRD) method. When electromagnetic radiation strikes on crystalline solid, X-ray diffraction impact occurs and when X-ray beam interacts with

an atom, electrons begin to oscillate at the identical frequency with the beam. Constructive interference occurs because the atoms in a crystalline structure are arranged in regular order (Van Heerden and Swanepoel 1997).

When conditions provide Bragg's Law ($n\lambda = 2d\sin\theta$) and well-defined X-ray beams separate the crystal structure in different directions. In the Bragg's Law, (λ) is electromagnetic radiation wavelength, (θ) is diffraction angle and (d) is a lattice spacing in the crystal structure (Rossi 2001).

When scanning the sample in the 2θ angle range, the diffractogram of the crystal structure is obtained in all possible direction. The crystallographic structure can be determined to compare with the reference sample in the database memory.

XRD studies of thin film samples were performed with Philips X'pert XRD device under conditions of 40 kV and 40 mA using Cu-K α radiation ($\lambda=0.154$ nm). Data was collected between the $20^\circ < 2\theta < 90^\circ$. The diffraction results were collected about 15 minutes for each thin film samples.

3.6. Surface Characterization

Scanning electron microscopy (SEM) studies of thin film samples were performed at 15 kV with FEI QUANTA 250 FEG and Philips XL 30S FEG device.



Figure 3.8. SEM instrument in IZTECH

3.7. Contact Angle Measurement

Contact angle measurement instrument (Attention Theta) give information about surface hydrophilicity of the thin films. Ultra-pure distilled water is used as a reference liquid. A 5 μL water droplet was set that is injected on the surface of the thin film with user manual in this analysis. This optical tensiometer is shown Figure 3.9.

High resolution (CCD) camera is using in the system. It catches the image of the water droplet at regular intervals and is then it is analyzed using the image in analysis software.



Figure 3.9. Contact angle measurement instrument in IZTECH

3.8. Surface Resistivity Measurement

Surface resistivity is an evaluation of the sample's connatural resistance to current flow. Physical dimensions of the sample are not important to measure surface resistivity. Unit for the surface resistivity is Ω/\square . Surface resistivity is measured by using two or four-point probe method is shown Figure 3.10 (Sze 2002).

This method uses linearly arranged probes that contact the surface of the test sample. The measurement of surface resistance by four probes dates back to 1916, and Wenner mentioned using this technique to measure the resistivity of the World (*John Willey & Son*, 1990). Four-point methods use additional two probes to measure the voltage potential of the sample. These probes do not have any current.

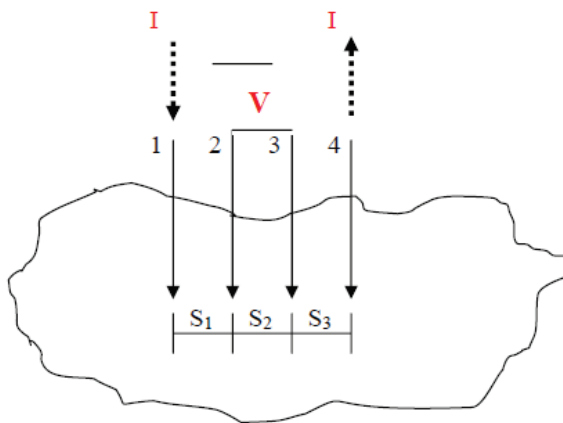


Figure 3.10. Probe 1 and 4 transport current (I), 2 and 3 evaluate voltage (V)
(Source: Gutiérrez, Li, and Patton 2002).

Generally, surface resistivity evaluation can be made on thin film samples or wafer of semiconductor. When measurements are made on infinite areas, correction factors should be used according to the sample geometry.

Correction factors depend on thickness and edge effect and location of the probe of the material. A high-quality four-point probe is required to achieve repeatable and reliable resistivity values. When measuring low resistivity samples, high currents are required to obtain good voltage in the current probes (Gutiérrez, Li, and Patton 2002).

3.9. Thickness Measurement

The thin film thickness is another important parameter of the limiting factor. Film thickness is directly proportional to the coating time. The photocatalytic activity is non-linearly dependent on the film deposition time (or film thickness). Studies have shown that photocatalytic activity does not increase for thicker film growth (5-15 μm) (Jung et al. 2005). Hiroaki Tada et. al. were studied TiO_2 thin film with a thickness between 50 and 200 nm. According to their results, photocatalytic activity reached a maximum level at 140 nm, after that it remained constant (Tada 1997). Looking at another study of H.J Nam et. al., thin film activity is reached saturation 360-420 nm of the thickness (Nam et al. 2004). These results indicate that photocatalytic activity is not dependent on the film thickness directly. It depends on the experimental techniques of the thin film preparation and set-up of the photocatalytic activity testing.

In the fact that film thickness influences the photocatalytic activity. Because, film (TiO_2) thickness increases, surface roughness is also increased. That's why incoming light is not absorbed through the film depth and photochemical reaction area between film and impurity is increased and is lowered photocatalytic activity.

Film thickness on the substrate is controlled by the shutter in DC magnetron sputtering system, it provides optimize thickness control and well quality on the surface of the film. The photoresist is used to remove a small area of the film on the specifics on the substrate. In this way, well is formed between film and substrate. Profilometer as shown in Figure 3.11. (Veeco DEKTAK 150 Profilometer) is used to trace topography along the path of the film and substrate.

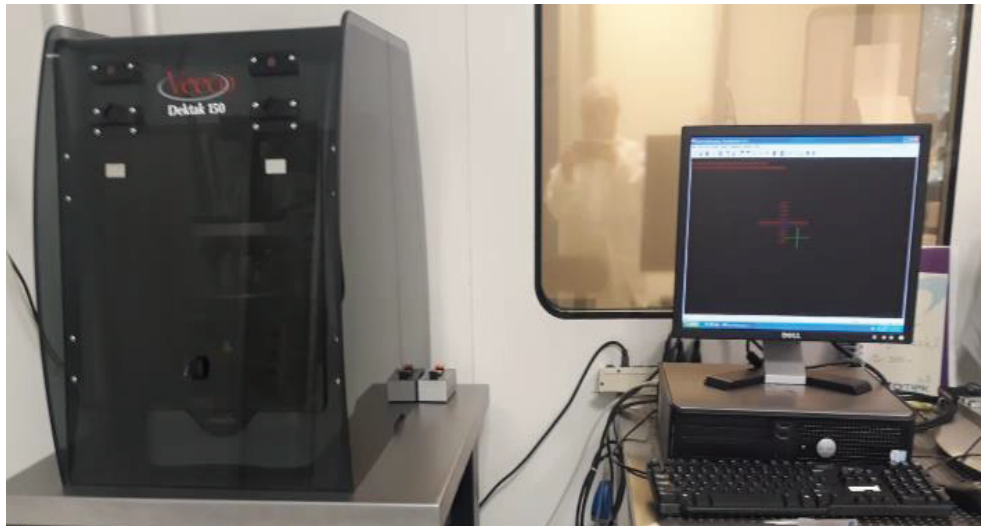


Figure 3.11. Profilometer instrument in IZTECH

CHAPTER 4

RESULTS & DISCUSSION

In this section, undoped TiO₂ and Ru-doped TiO₂ thin films were characterized using these techniques such as Film Thickness, SEM, EDX, Raman and XRD analysis.

4.1. Film Thickness

The film thickness was determined by Profilometer (Veeco DEKTAK 150 Profilometer). To evaluate the reproducibility of the film, the thickness of all films were measured. Data XY chart measurement and thickness data of undoped and Ru-doped TiO₂ are shown Figure 4.1. The average thickness of thin films is nearly 50 nm.

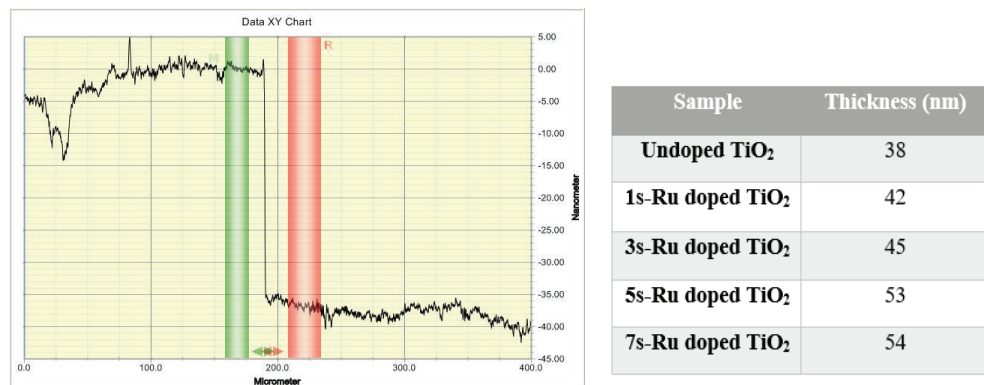


Figure 4.1. Data XY Chart measurement and thickness data of undoped and Ru-doped TiO₂

Low thickness of thin films provides good absorption ability and transmission was reached nearly 75% in the spectral region (450nm-550nm), which is a significant region in solar cell application.

Due to the magnetron sputtering technique, thin film thickness has been optimized properly.

4.2. Optical Characterization

The change in transmission analysis obtained from the UV-Vis spectrophotometer. In this study, optical properties of undoped and Ru-doped TiO₂ were obtained due to a PerkinElmer Lambda 950 UV/VIS/NIR spectrophotometer with wavelength range between 200-2600 nm.

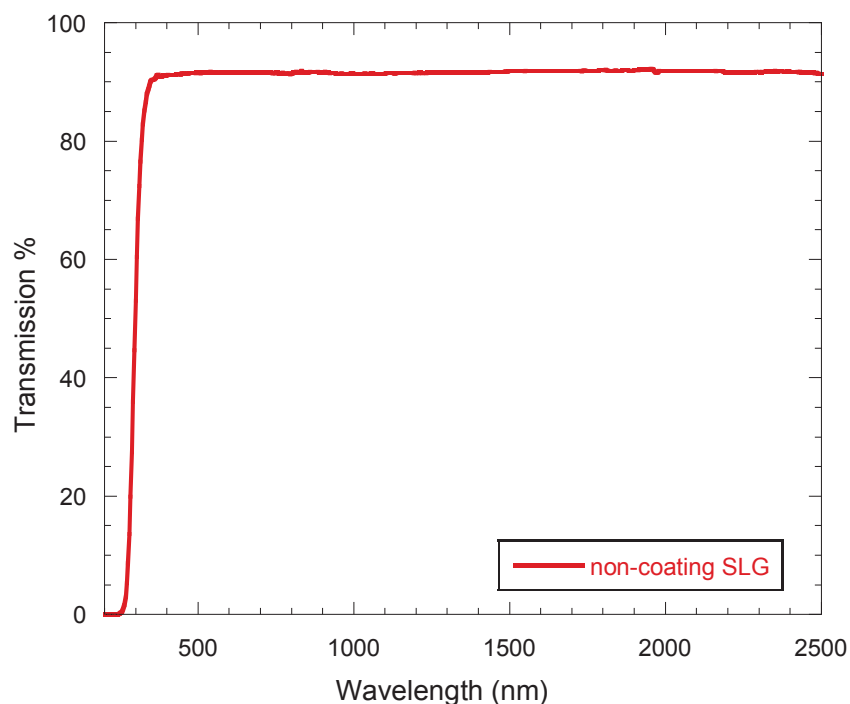


Figure 4.2. UV-Vis spectrophotometric analysis of uncoated soda lime glass

The transmission of glass substrate was approximately 90% in spectral range as shown in the Figure 4.2.

The optical transmission values of the glasses used as substrate material were found to be suitable for characterization studies.

The optical properties of the coating layer play a huge role in solar cell performance. Coating speed and film thickness have been optimized in previous studies. As known from the literature, the film thickness increases with increasing coating speed, and the homogeneity of the films is deteriorated. In Figure 4.3. transmission is higher at 480 nm-660 nm. It provides more advantages for solar cell applications. When look at IR region in spectrum, transmission is getting lower, this properties of the thin film prevents the surface from overheating.

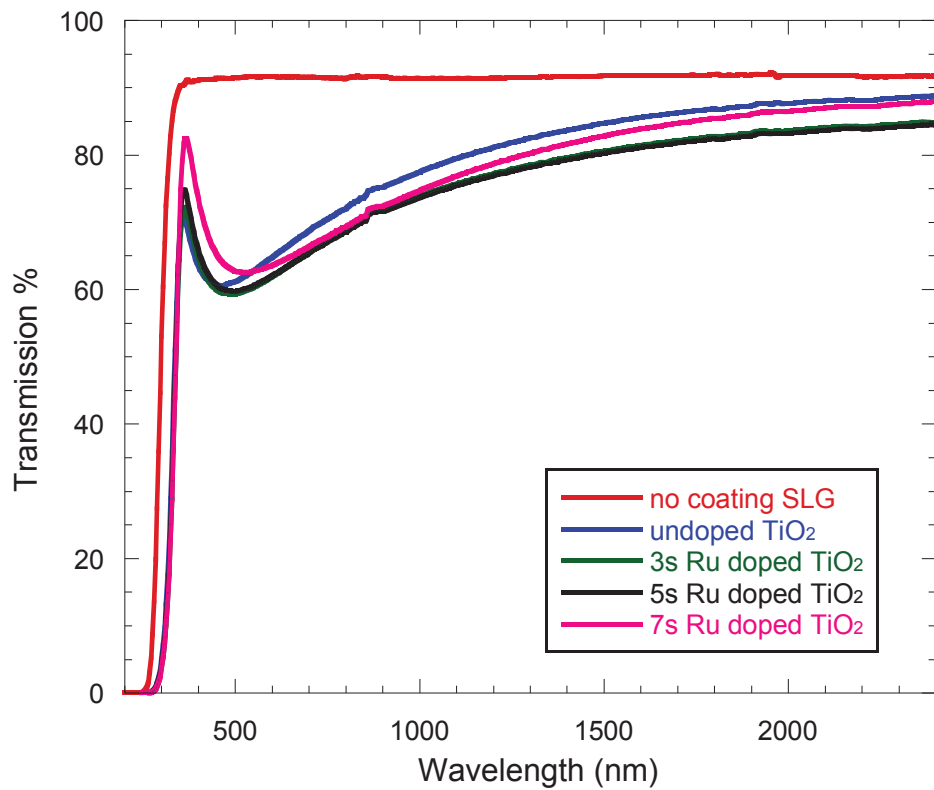
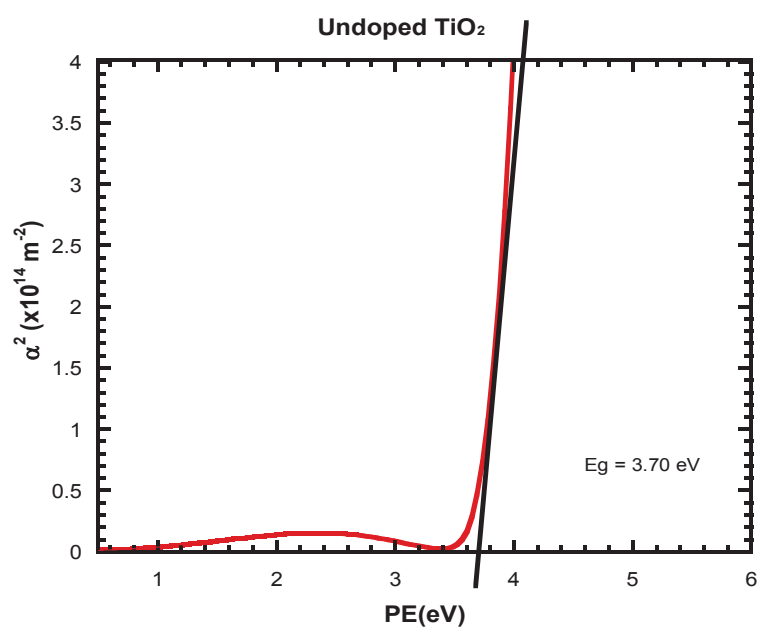


Figure 4.3. UV-vis analysis spectrophotometric analysis of undoped and Ru-doped TiO₂

When looking at the graph, the transmittance of non-doped TiO₂ thin film and 3 sec, 5 sec and 7 sec Ru doped TiO₂ thin films samples are higher than 70%. In this way, it can supply the enough transmissivity of cover part of solar cells (Nukaya et al. 2002). Transmissivity can be regulated by changing the thickness of the thin films according to application areas. Ru-doped TiO₂ coating soda-lime glass substrate is not compromised its optical properties.

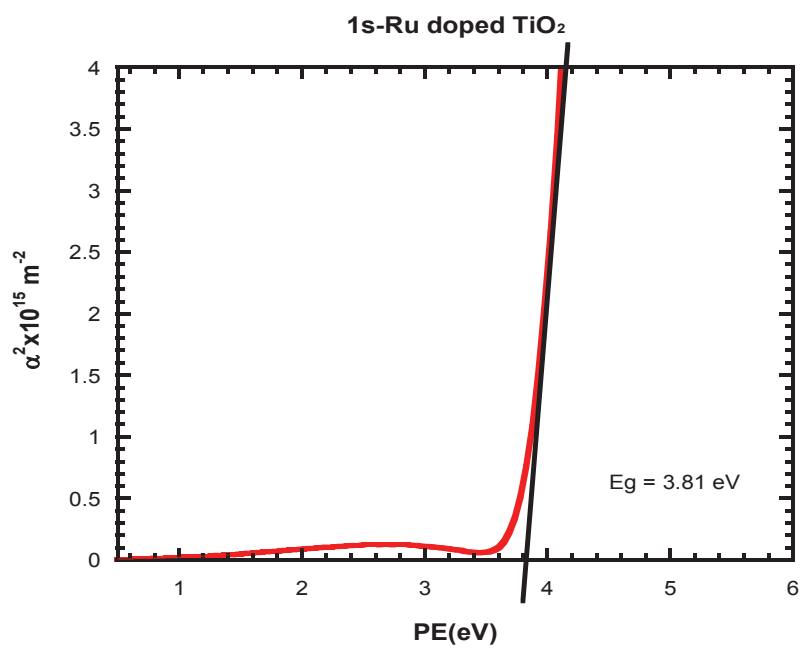
4.3. Band Gap Energy

The band gap energy for undoped and Ru-doped TiO₂ thin film on soda-lime glass substrate was calculated by using Tauc law as mentioned in the section 2.8. The band gap energy of the coated samples are shown in the Figure 4.4.(a-e). The band gap energy values are listed in the Table 4.1.



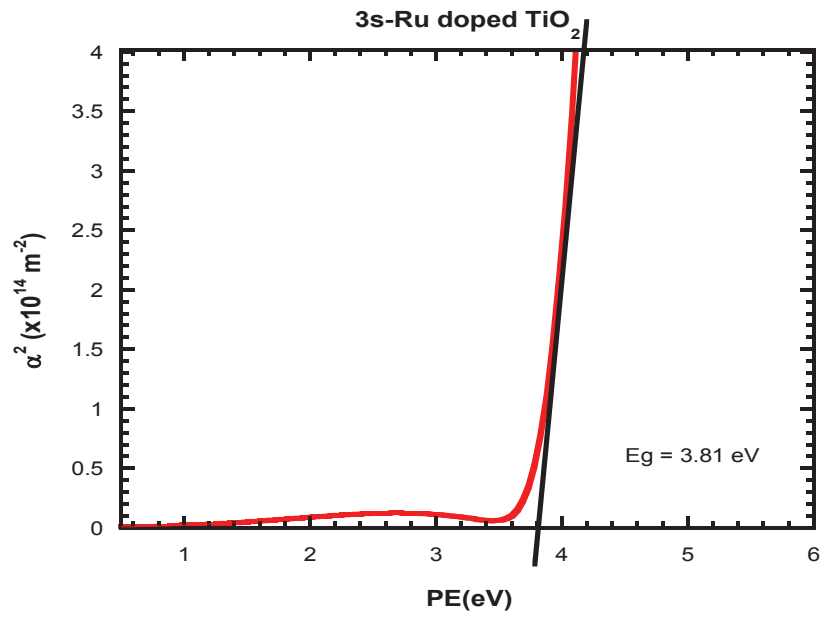
(a)

Figure 4.4a. Band gap energy for the undoped TiO₂



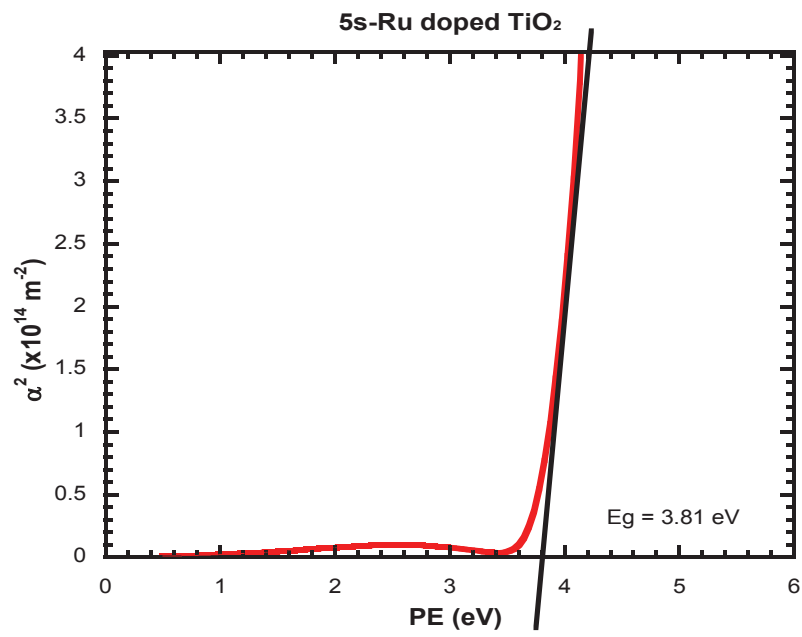
(b)

Figure 4.4b. Band gap energy for the 1s-Ru doped TiO₂



(c)

Figure 4.4c. Band gap energy for the 3s-Ru doped TiO₂



(d)

Figure 4.4d. Band gap energy for the 5s-Ru doped TiO₂

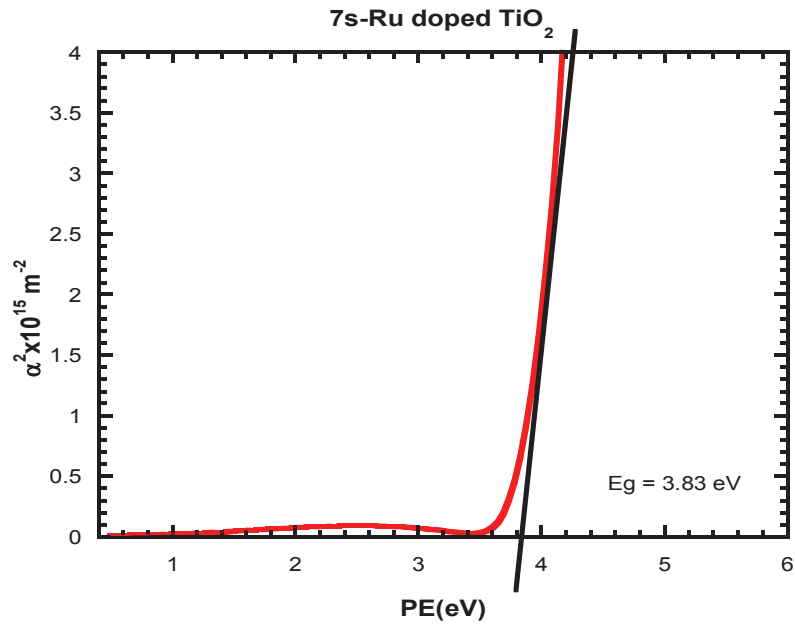


Figure 4.4e. Band gap energy for the 7s-Ru doped TiO₂

Table 4.1. Values of the band gap energy of the undoped and Ru doped TiO₂ thin films samples

Sample	Band Gap Energy (eV)
Undoped TiO ₂	3.70
1s-Ru doped TiO ₂	3.81
3s-Ru doped TiO ₂	3.81
5s-Ru doped TiO ₂	3.81
7s-Ru doped TiO ₂	3.83

From the table 4.1., while the quantity of the ruthenium doping increase, the crystallization is affected in the formation of the band gap energy. Ruthenium ions may be changed to the localized states resulting from the increase in the physical crystal defects of the thin film with the increasing of the time, which leads to increment in the band gap energy (Peerakiathajohn et al. 2011).

If band gap energy is reduced, photocatalytic activity will be increased under visible region of the solar spectrum. This reducing band gap energy makes it possible to use the photocatalyst in sunlight without the need for UV lamps (Abdulkareem et al, 2013).

4.4. XRD Analysis of Undoped and Doped TiO₂ Thin Films

XRD analysis was performed to detect the secondary phases transformation and investigate the quality of the crystalline structure. According to the XRD scans, 2θ degrees between 10° - 90° were investigated. As a result of the XRD measurements, the 2θ value of all films approximately 25.38° which were calcined at 500°C . Considering the references ($2\theta = 25,39^\circ$ (101), $37,89^\circ$ (004), $48,1^\circ$ (200), $54,005^\circ$ (105) and $55,18^\circ$ (211) are the anatase phase peaks), shows that this peak indicates the presence of the anatase phase (Jameel, Haider, and Taha 2013). The TiO₂ thin films which were doped with Ru⁺ formed the anatase phase at a temperature of 500°C while the amorphous structure occurred in the non-heat treated. Figure 4.5. shows the XRD spectrum of undoped and ruthenium doped TiO₂ thin film on SLG substrate.

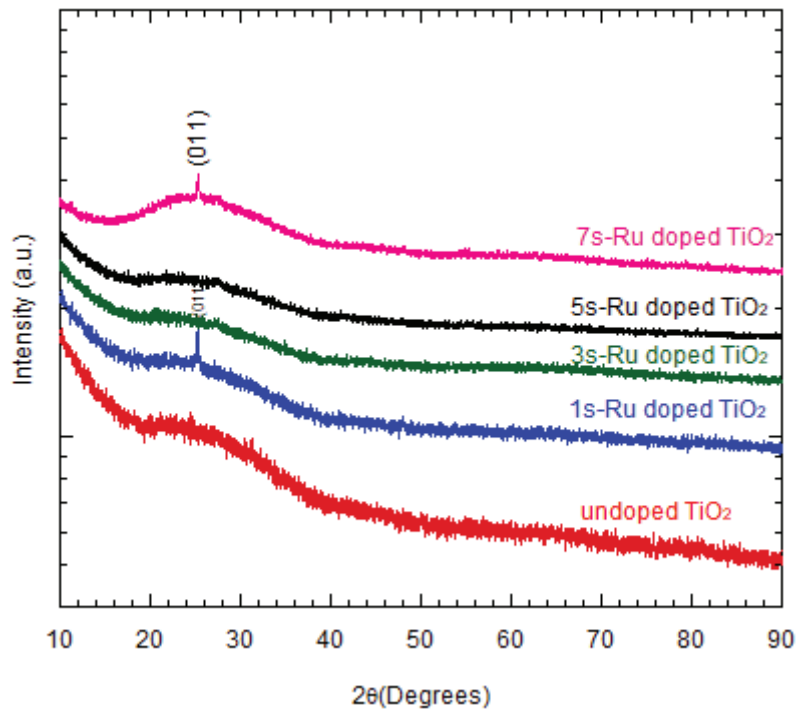


Figure 4.5. XRD pattern of undoped and Ru doped TiO₂ thin films samples

All thin films were heat-treated at 500°C for 2 hours. It is observed that nearly sharp peak detected at $25,39^\circ$ only 1s and 7s Ru-doped TiO₂ sample. All of the thin films were amorphous except 1s Ru-doped and 7s- Ru doped thin films as seen in Table 4.2.

Table 4.2. XRD results of undoped and Ru-doped TiO₂ thin films samples

Sample	T (°C)	t (min.)	Phase (XRD)
Undoped TiO ₂	500	120	Amorphous
1s-Ru doped TiO ₂	500	120	Anatase
3s-Ru doped TiO ₂	500	120	Amorphous
5s-Ru doped TiO ₂	500	120	Amorphous
7s-Ru doped TiO ₂	500	120	Anatase

4.5. Atomic Force Microscopy (AFM) Results

Atomic force microscopy is used to evaluate surface roughness and morphology of optimized undoped TiO₂ and Ru-doped TiO₂ samples. Figure 4.6. and Figure 4.7. show the (3D) image and the histogram of the sample respectively. These images show that; the formations of thin films consist of non-uniform grain size. The root mean square (Rms) value is used to represent the roughness. The root mean square (Rms) value is equal to 2.04 nm for undoped TiO₂ thin films and 1.77 nm for Ru-doped TiO₂ thin films. Surface roughness is important for photocatalytic activity. Because, it provides to increment of surface area. The surface area and photodegradation efficiency is directly proportional.

a)

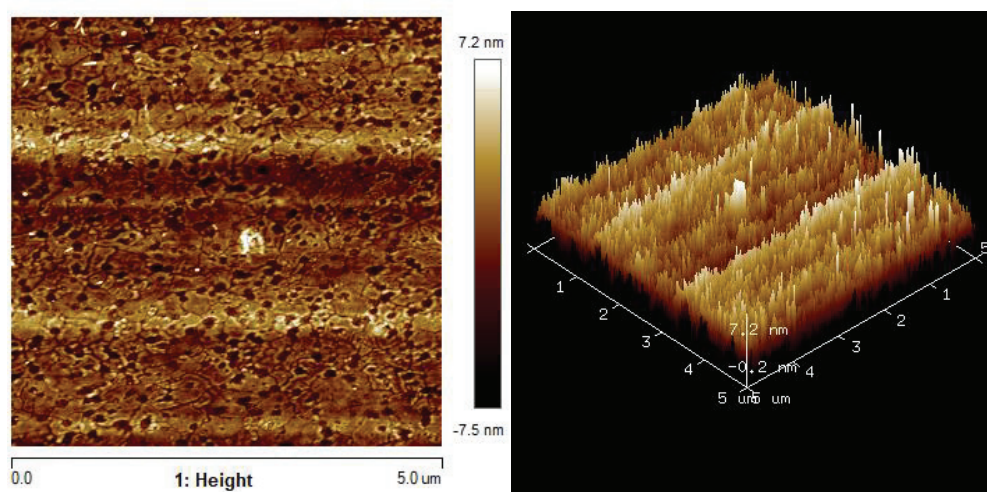
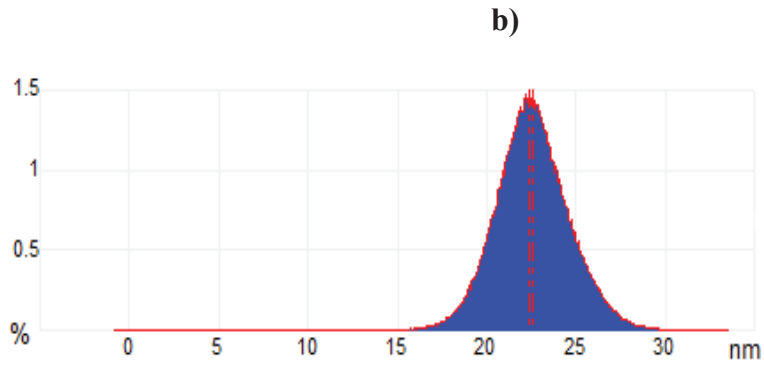


Figure 4.6a. 2-D and 3-D AFM image for the undoped TiO₂ thin films



Sample	Minimum Peak Depth	Maximum Peak Depth	Rms Rough(Rq)	Ave Rough(Ra)	Image R _{max}
Undoped TiO ₂	21.4547nm	22.6nm	2.04 nm	1.59 nm	32.7 nm

Figure 4.6b. Undoped TiO₂ thin films AFM histogram

Surface roughness of Ru-doped TiO₂ thin film is lower than undoped TiO₂ thin film. When Ru⁺ ions were doped in TiO₂ thin films, the film surface became smoother. In this way, transmission of the surface increased. This thin film can be used as the upper surface of the solar panels due to its high transparency and do not prevent absorption of the sunlight.

a)

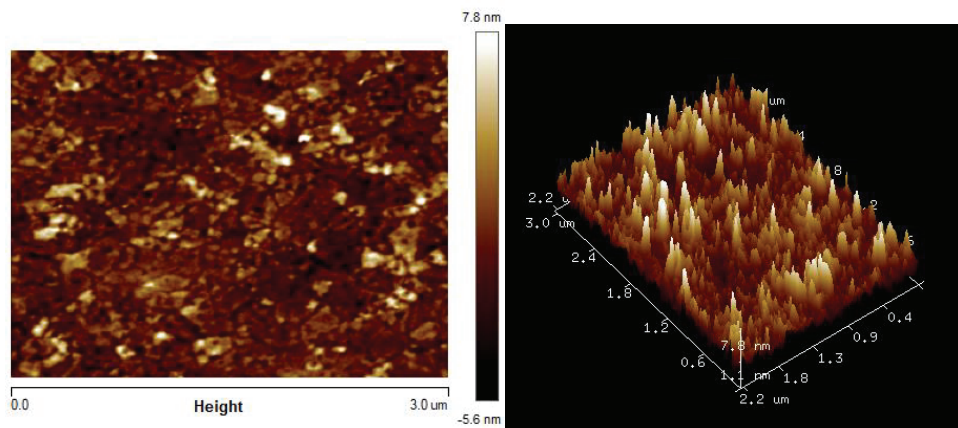
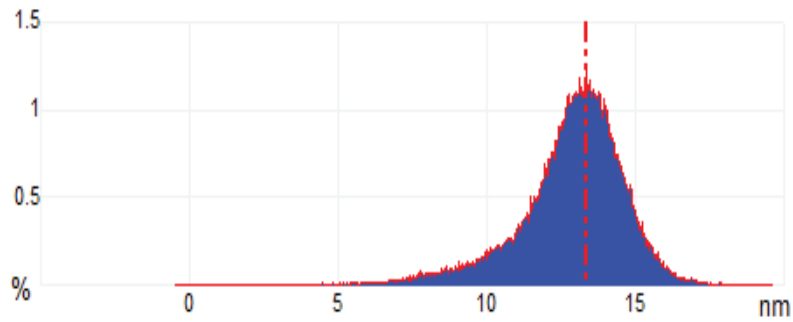


Figure 4.7a. 2-D and 3-D AFM image for the Ru-doped TiO₂ thin films

b)



Sample	Minimum Peak Depth	Maximum Peak Depth	Rms Rough(Rq)	Ave Rough(Ra)	Image R _{max}
Ru-doped TiO ₂	12.3085nm	13.3nm	1.77nm	1.32nm	19.1nm

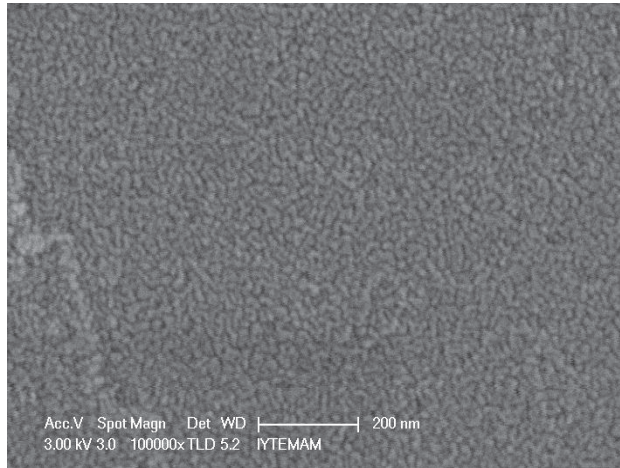
Figure 4.7b. Ru-doped TiO₂ thin films AFM histogram

4.6. SEM Analysis of Undoped and Ru-doped TiO₂ Thin Films

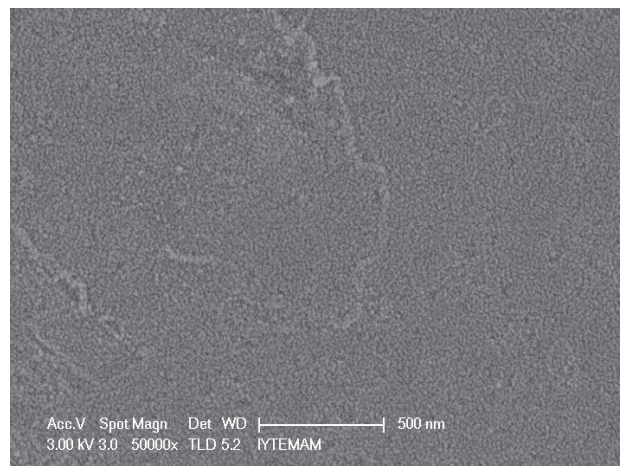
In-depth morphological analysis for the undoped TiO₂ and Ru-doped TiO₂ thin films were observed with powerful technique Scanning Electron Microscope (SEM) (Hamzah et al. 2012). According to the SEM images of the thin films deposited on Ru-doped TiO₂ substrate which was seen in Figure 4.8. and Figure 4.9. Each film was heat-treated at 500°C after coating. From the results of the SEM analysis, it is seen that the coated films are very similar as a structure. The cracks seen in the images belong to the soda lime glass which is the substrate material. These cracks occurred when preparing the sample for SEM analysis.

After the SEM analysis of the film, EDX method was used for elemental analysis of doping metal of Ru into TiO₂ crystal structure.

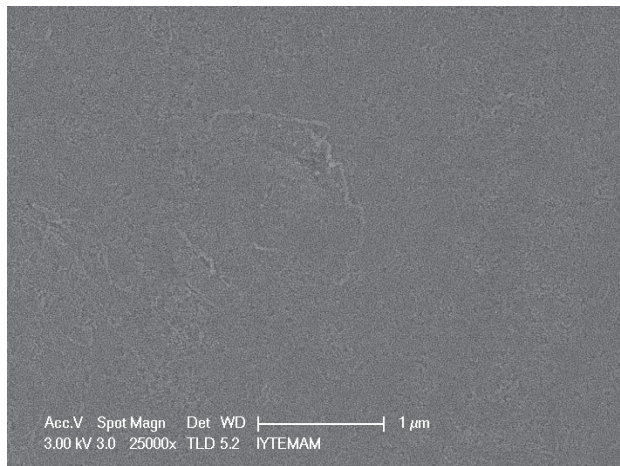
The EDX analyses were performed on a selected region of the SEM images and the results were obtained as average Wt% and Atomic%. The Ru⁺ ions were determined in the TiO₂ crystal structure between in the Figure 4.10 and the Figure 4.14. EDX scans were performed 10 μm² to include several grains. When look at at the average elemental compositions of undoped and Ru-doped TiO₂ thin films, Wt% and At% were increased gradually. Si ratio of thin film from SLG was decreased. Furthermore, it was observed that the amount of Ti ratio increased when EDX results were examined.



(a)

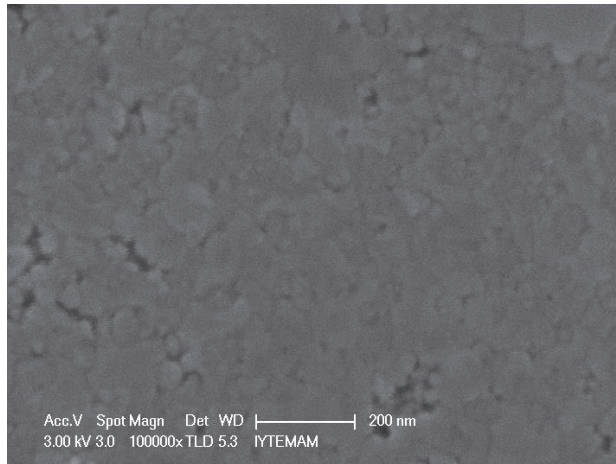


(b)

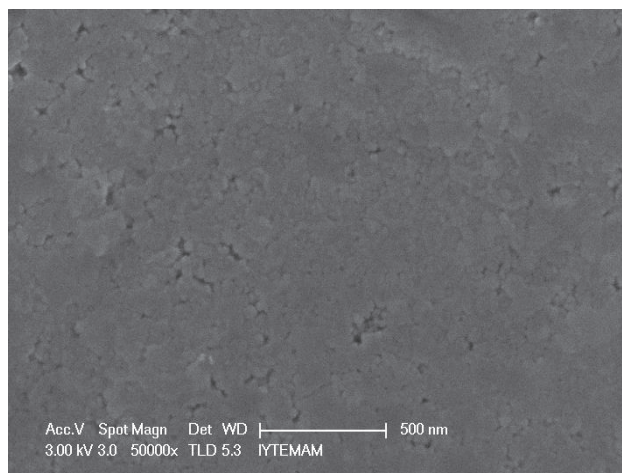


(c)

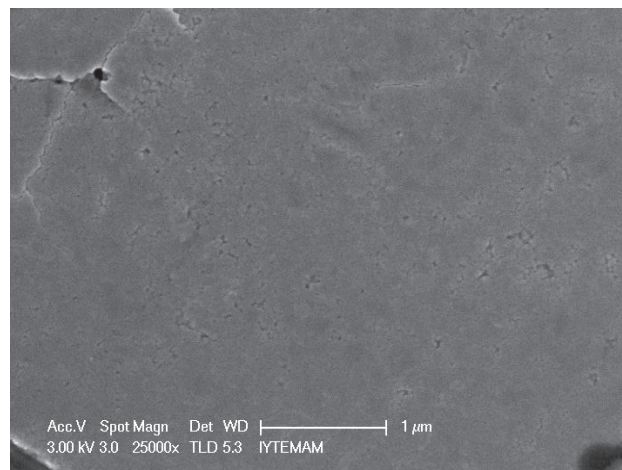
Figure 4.8. (a), (b) and (c) SEM images of undoped TiO₂ thin films



(a)

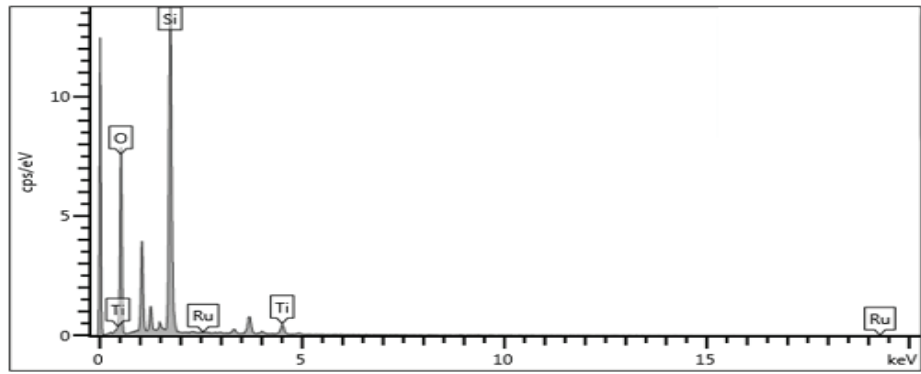


(b)



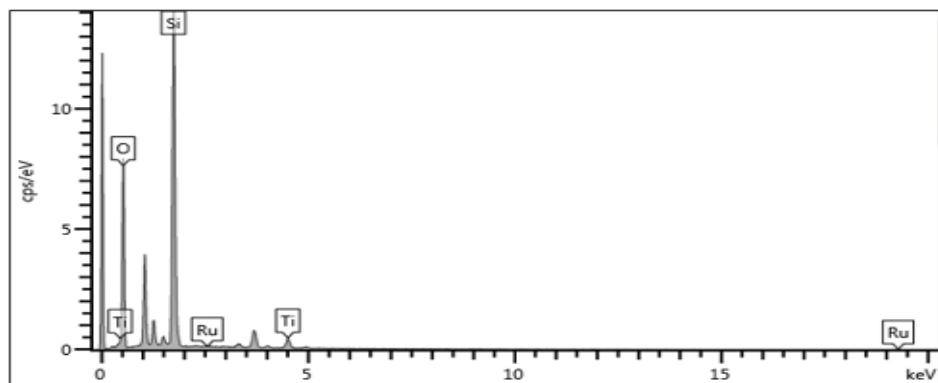
(c)

Figure 4.9. (a), (b) and (c) SEM images of Ru-doped TiO₂ thin films



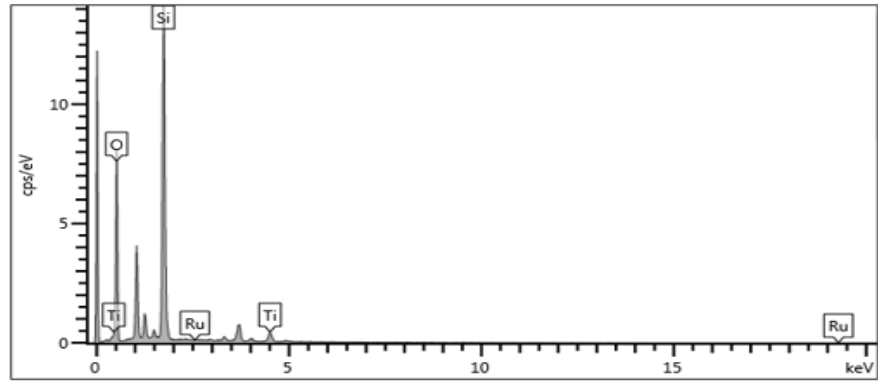
Element	Wt%	Atomic %
O	55.78	69.81
Si	39.67	28.29
Ti	4.55	1.90
Ru	0.00	0.00
Total:	100.00	100.00

Figure 4.10. Undoped TiO₂ thin film EDX spectrums



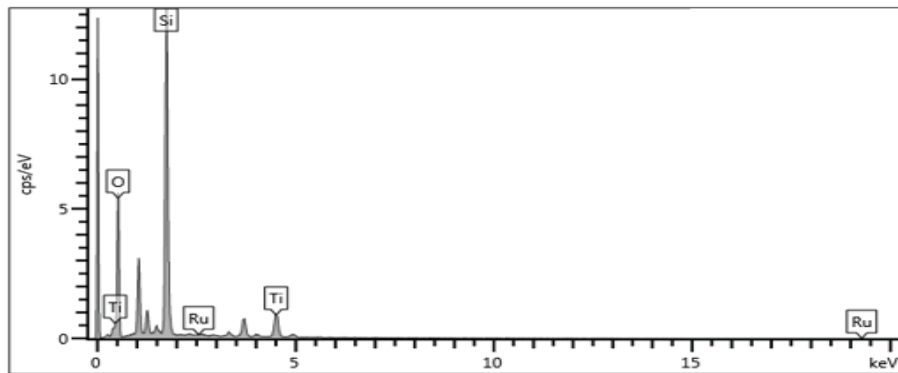
Element	Wt%	Atomic %
O	55.89	69.90
Si	39.61	28.22
Ti	4.50	1.88
Ru	0.00	0.00
Total:	100.00	100.00

Figure 4.11. 1s-Ru doped TiO₂ thin films EDX spectrums



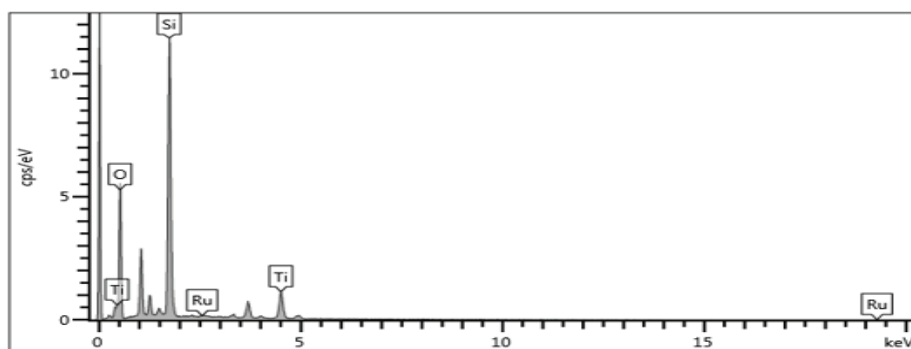
Element	Wt%	Atomic %
O	55.95	69.97
Si	39.55	28.18
Ti	4.40	1.84
Ru	0.10	0.02
Total:	100.00	100.00

Figure 4.12. 3s-Ru doped TiO₂ thin films EDX spectrums



Element	Wt%	Atomic %
O	50.80	66.73
Si	37.93	28.38
Ti	11.05	4.85
Ru	0.22	0.05
Total:	100.00	100.00

Figure 4.13. 5s-Ru doped TiO₂ thin films EDX spectrums



Element	Wt%	Atomic %
O	51.78	68.21
Si	34.60	25.96
Ti	12.92	5.68
Ru	0.70	0.15
Total:	100.00	100.00

Figure 4.14. 7s-Ru doped TiO₂ Thin Film EDX Spectrum

(EDX) element analysis results (%) showed that Ru⁺ ions were determined in the selected regions for analysis on the Ru-doped TiO₂ film surface, and as the amount of Ru⁺ ion increased, the Wt% and Atomic % amount of Si ions decreased respectively in the analysis.

4.7. Contact Angle Results

Contact angle measurements were applied under air setting control to using the manual-drop method as it was clarified before. This figure shows that undoped TiO₂ thin film contact angle 47.309° and Ru-doped TiO₂ thin film contact angle 63.218°. According to results ruthenium doping reduces the hydrophilic property slightly but the thin film does not lose the hydrophilic property. If contact angle equals (0°), this thin film reaches superhydrophilic property. These results were obtained without exposure UV radiation. If TiO₂ thin film exposes UV radiation before measure contact angle, irradiated electrons reduce the Ti⁺⁴ to hydrophilic Ti⁺³, photo-irradiated holes oxidize O⁻² groups and occur oxygen vacancies. These vacancies are filled with water molecules that produce absorbed OH groups and enhance the hydrophilic properties of the surface. That's why the surface expose UV radiation, contact angle approaches 0° (Nishimoto and Bhushan 2013).



Thin Film Group	Contact Angle (°)	Images
Undoped TiO ₂	47.309°	
Ru-doped TiO ₂	63.218°	

Figure 4.15. Contact angle results of undoped TiO₂ and Ru-doped TiO₂ thin films

4.8. Surface Resistivity Measurement

The resistivity of the undoped and Ru-doped TiO₂ thin film was measured four-probe method and correction factor is used as 4.5324.

Table 4.3. Resistivity values of undoped and Ru doped TiO₂ Thin Films

Sample	Resistivity (Ω / \square)	
	nonannealed	annealed(500°C)
Undoped TiO₂	-	-
1s-Ru doped TiO₂	40.7 k Ω/\square	-
3s-Ru doped TiO₂	-	-
5s-Ru doped TiO₂	22.6 k Ω/\square	14.0 k Ω/\square
7s-Ru doped TiO₂	9.51 k Ω/\square	4.9 k Ω/\square

From the table 4.3., Ru-doped TiO₂ shows high resistivity and of course low conductivity. According to the table, when the ratio of ruthenium increases in the TiO₂ thin film, the resistivity decreases respectively. When the sample was annealed at 500 °C for 2 hours, it could be changed crystal structure of the thin film and it is observed that

resistivity could be decreased. The electrical properties of TiO₂ can be interesting because of gas sensor applications (Sankar and Gopchandran 2009).

The resistivity of the undoped and Ru-doped TiO₂ thin film was measured four-probe method and the correction factor is used as 4.5324.

Rs was calculated $R_s = (4.5324 * V) / I$. by this formulation.

4.9. Photocatalytic Activity

TiO₂ thin films preparation and photocatalytic activity investigation of using Methylene Blue dye as a pollutant procedure was explained in Chapter 3.3. in detailed.

The thin films photocatalytic activities were detected by decomposition of organic pollution of cationic thiazine dye methylene blue under Ultraviolet Light (UV) illumination. Methylene Blue maximum absorption peaks at 664.5 nm, 614 nm 292 nm and 246 nm. The peak of 664.5 nm indicates Sulphur-Nitrogen conjugated system. The peaks of 246 nm and 292 nm exhibits phenothiazine forms in the MB molecules (Tio 2018).

In this study, undoped TiO₂ and Ru doped TiO₂ were prepared by DC magnetron sputtering technique. Undoped TiO₂, 1s-Ru doped TiO₂, 3s-Ru doped TiO₂, 5s-Ru doped TiO₂ and 7s-Ru doped TiO₂ were placed different beakers. Each beaker contained 15 ml MB solution as an organic contamination. Before starting photocatalytic degradation test MB solution was measured as a reference to observe decreasing intensity of absorbance values. Reference value should be 1 nearly. Nearly, 2.5 ml of the solutions were taken with pasteur pipette and initial absorbance values were measured for every MB solution after exposed UV light. The solution was poured back into the beaker. After 1 hours, 3 hours, 5 hours and 24 hours later, degradation of MB solution was calculated as a percentage.

The Absorbance of all thin film samples did not achieve zero value even after 24 hours of irradiated UV light.

Absorbance decay of methylene blue versus (200-1000 nm) wavelength interval of different ratios Ruthenium (Ru⁺) doped TiO₂ thin films degradation effect were illustrated through Figure 4.16. to the Figure 4.20.

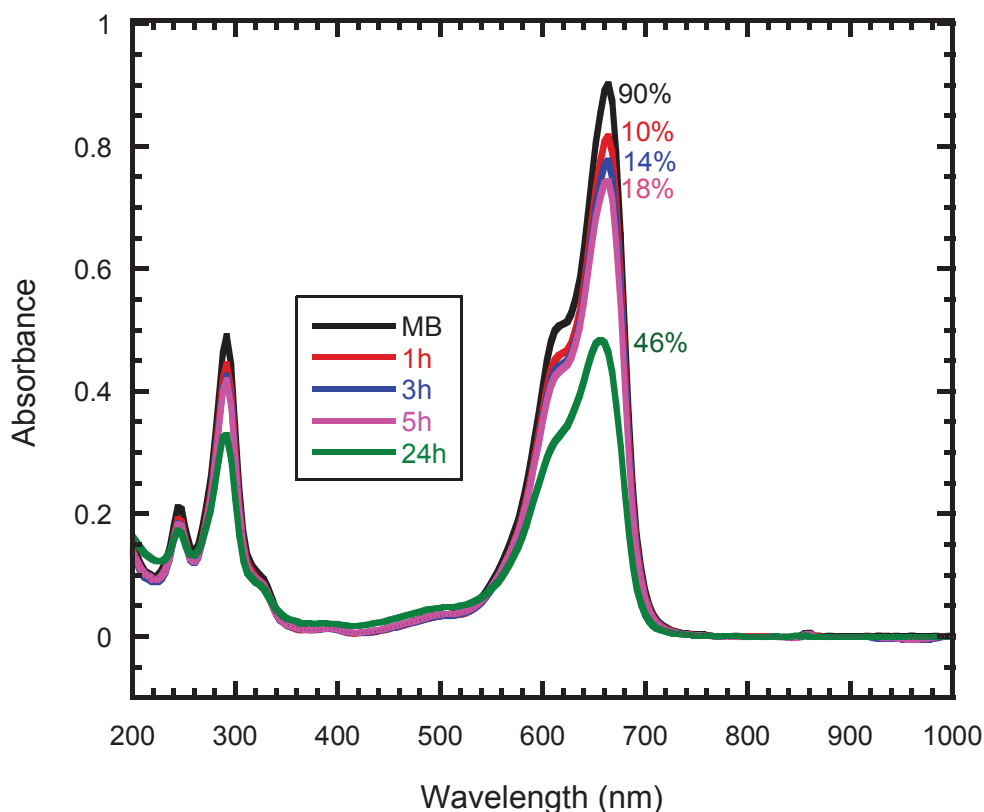


Figure 4.16. Photocatalytic degradation of Methylene Blue solution (10^{-5} M) with undoped TiO_2 catalyst

Methylene Blue (MB) solution (15 ml) with undoped TiO_2 thin film (2 cm X 2 cm) which in the bottom of the beaker was illuminated by UV source (Philips TUV 16W GJ6 T5) 20 cm away and spectral range is 200-400 nm with 1st-3rd-5th and 24th hours respectively. Due to irradiated TiO_2 thin film catalyst, nitrogen and sulphur conjugated structure was destroyed gradually. The peak of 664 nm shows Sulphur-nitrogen conjugated system. Depends on this, solution color changed from dark blue to light blue. Top of peak in the Figure 4.16, methylene blue absorption is used as a reference solution and after 1 hours later, 10% of MB solution was degraded, after 3 hours later 14% of MB solution was degraded, after 5 hours later 18% of MB solution was degraded and lastly, absorption of MB solution was degraded about 46% at the end of the 24 hours using undoped TiO_2 thin film in MB solution under UV light. The concentrations can be calculated using absorbance values for every steps of MB solutions by Beer Lambert Law. When the absorbance values of MB decreases, the concentration value also decreases and color of the solutions discolored.

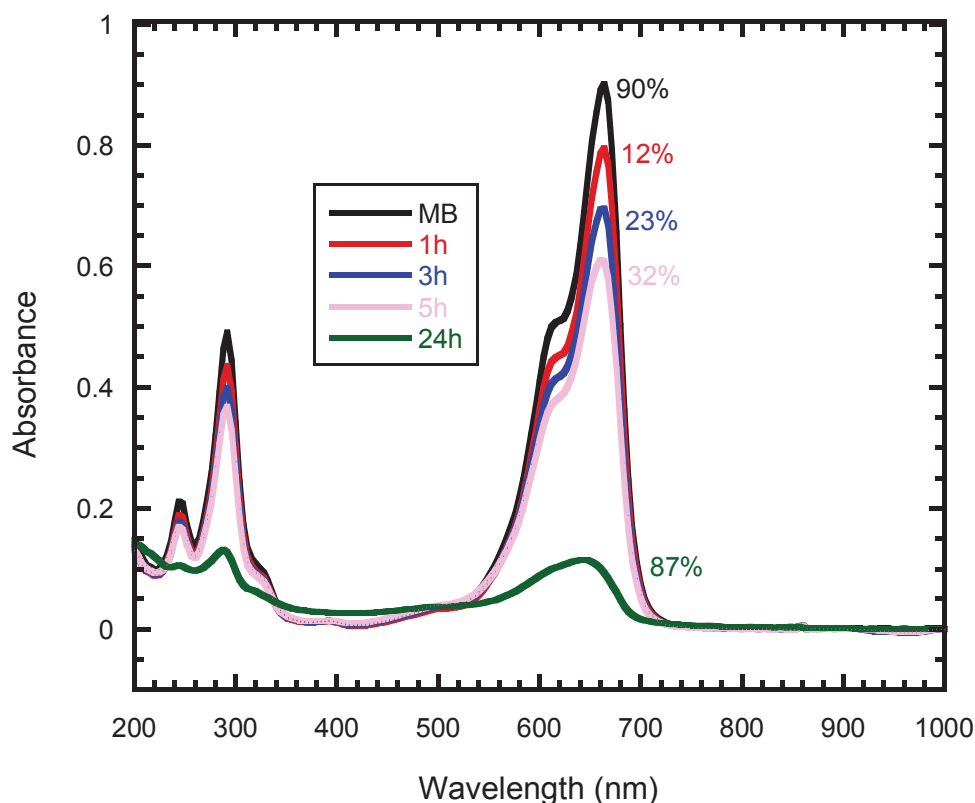


Figure 4.17. Photocatalytic degradation of Methylene Blue solution (10^{-5} M) with 1s-Ru doped TiO_2 catalyst

When looking at another graph, only 1s-Ru doped TiO_2 thin film was used. Top of the absorption peak MB at the same value. Methylene Blue solution was degraded 12% at the end of the 1st hour, 23% at the end of the 3rd hour, 32% at the end of the 5th hour and 87% of MB solution was degraded at the end of the 24th hour. 1s- Ru doped TiO_2 thin film has the highest photocatalytic activity performance with 7s-Ru doped TiO_2 thin film among other thin films.

It was seen that, considering the XRD results ($2\theta = 25,39^\circ$ (101), $37,89^\circ$ (004), $48,1^\circ$ (200), $54,005^\circ$ (105) and $55,18^\circ$ (211)), 1s-Ru doped TiO_2 and 7s-Ru doped TiO_2 have anatase peak. All thin films were heat-treated at 500°C for 2 hours. It is observed that nearly sharp peak detected at $25,39^\circ$ only 1s and 7s Ru-doped TiO_2 sample. All of the thin films were amorphous except 1s Ru-doped and 7s- Ru doped thin films.

Anatase phase of TiO_2 more reactive when compared rutile and brookite phase of TiO_2 . It has been already proven that, anatase phase of TiO_2 higher photocatalytic activity.

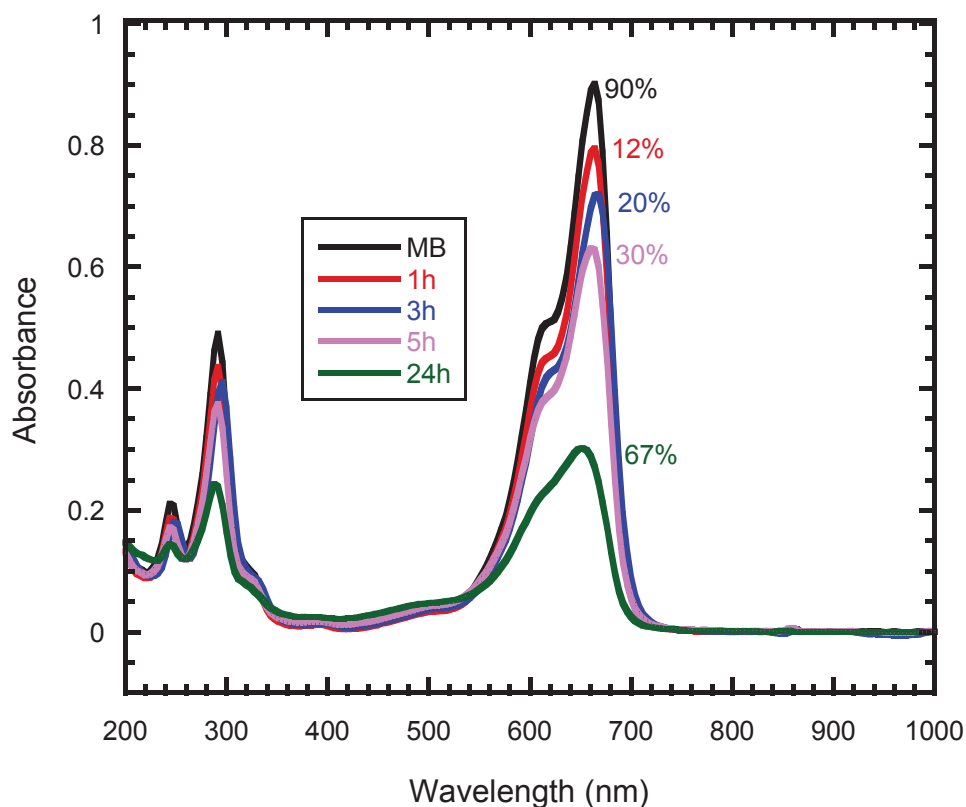


Figure 4.18. Photocatalytic degradation of Methylene Blue solution (10^{-5} M) with 3s-Ru doped TiO_2 catalyst

When look at the Figure 4.18., 3s-Ru doped TiO_2 thin film was used and all parameters are the same. Photocatalytic activity was changed as the ratio of the doping metal into the coated materials were changed. By decomposition of Sulphur-nitrogen conjugated structure of MB, the solution was degraded 12% at the end of the 1st hour, 20% of MB solution was degraded at the end of the 3rd hours, 30% of MB solution was degraded at the end of the 5th hours and 67% of MB solution was degraded at the end of the 24th hours.

Compared to XRD results, 3s-Ru doped TiO_2 has amorphous crystal structure. The fact that amorphous structure of material does not prevent photocatalytic activity. It only lowers the rate of the photocatalytic activity. Compared to anatase crystal structure, it seen that 3s-Ru doped TiO_2 thin film has lower photocatalytic activity.

The improvement of photocatalytic activity performance thin films could be heat treated again and the transfer of sodium ions from SLG to Ru doped TiO_2 thin film should be prevented. To enhancing surface area of thin films as solution to increase photocatalytic activity also.

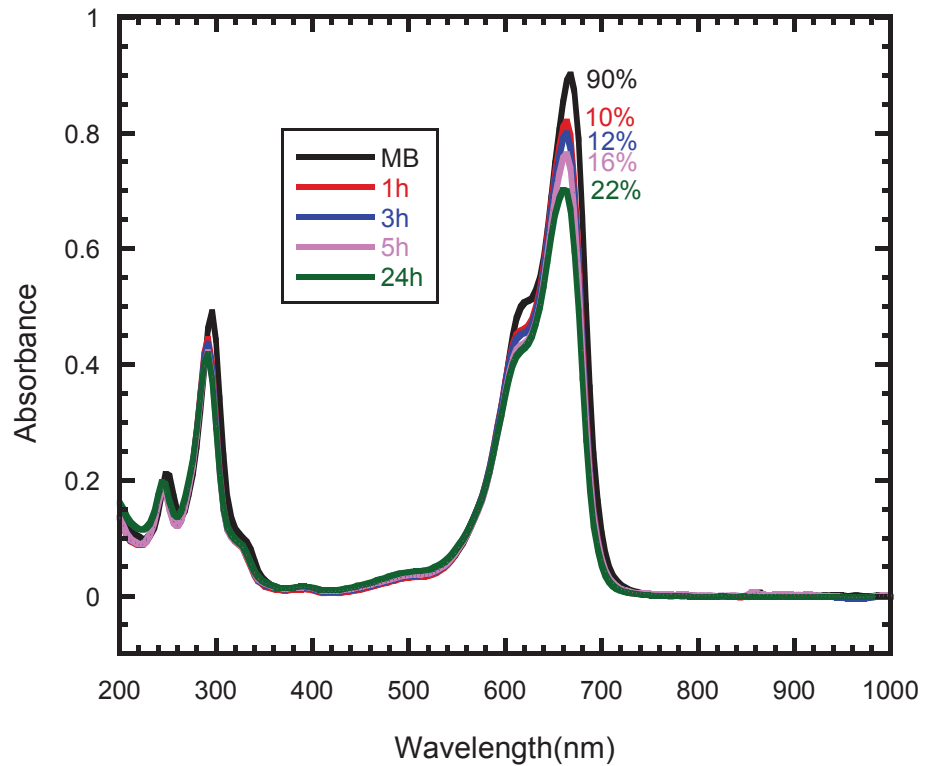


Figure 4.19. Photocatalytic degradation of Methylene Blue solution (10^{-5} M) with 5s-Ru doped TiO_2 catalyst

In the Figure 4.19., Methylene Blue solution was degraded 10% at the end of the 1st hour, 12% at the end of the 3rd hour, 16% at the end of the 5th hour and 22% of MB solution was degraded at the end of the 24th hour.

When looked at the XRD results, 5s-Ru-doped TiO_2 has amorphous crystal structure. Anatase phase of TiO_2 could not be obtained. Electron- hole recombination could be generated and therefore photocatalytic activity may be decreased. The lowest photocatalytic activity was obtained among all coated TiO_2 thin films. One of the reasons of the results, it could not be exposed to light evenly under UV light.

Since the thickness of the coated thin films is approximately 50 nm, so it may be reversed into the MB solution. Also sodium ion transfer could be occurred from SLG to thin films. Increasing the thickness, porosity and surface area of thin film are important features to increase photocatalytic activity.

When considering the planned application of TiO_2 thin film, the increment of thickness and porosity can decrease the absorption of light in solar panels and prevent sufficient energy production.

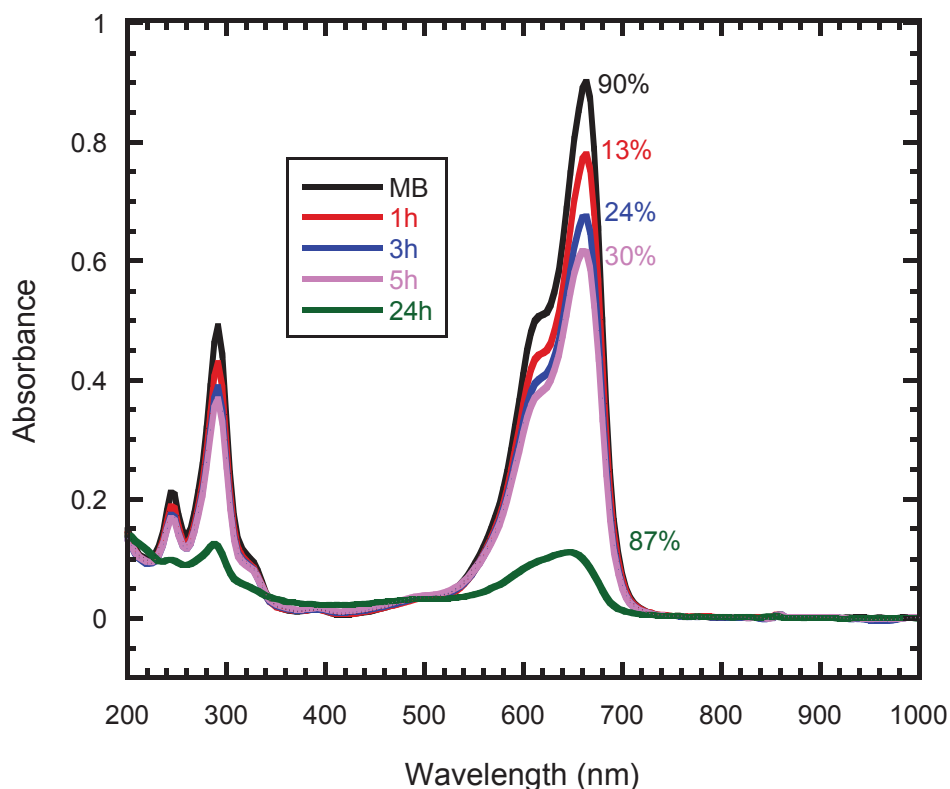


Figure 4.20. Photocatalytic degradation of Methylene Blue solution (10^{-5} M) with 7s-Ru-doped TiO_2 catalyst

The last Figure 4.20., Methylene Blue solution was degraded 13% at the end of the 1st hour, 24% at the end of the 3rd hour, 30% at the end of the 5th hour and 87% of MB solution was degraded at the end of the 24th hour.

It was mentioned 1s-Ru doped TiO_2 , XRD results ($2\theta = 25,39^\circ$ (101), $37,89^\circ$ (004), $48,1^\circ$ (200), $54,005^\circ$ (105) and $55,18^\circ$ (211)), supported that 7-Ru doped TiO_2 have anatase peak as 1s-Ru doped TiO_2 based on reference. Although the intensity of the obtained peak was very small but photocatalytic activity was higher. If all the peaks of the XRD references were obtained in the crystal structure, the solution of methylene blue could be completely degraded and the solution could be becoming completely colorless. When compared with the more commonly used powdered form of TiO_2 in the literature, the superiority of the form of thin film has been proven by D.C magnetron sputtering.

Absorbance decay of Methylene blue (MB) solution versus UV irradiation time for the undoped and Ru-doped TiO_2 thin films are showed in the graph. From this graph, Methylene Blue absorbance declines exponentially with the increasing of UV irradiation time.

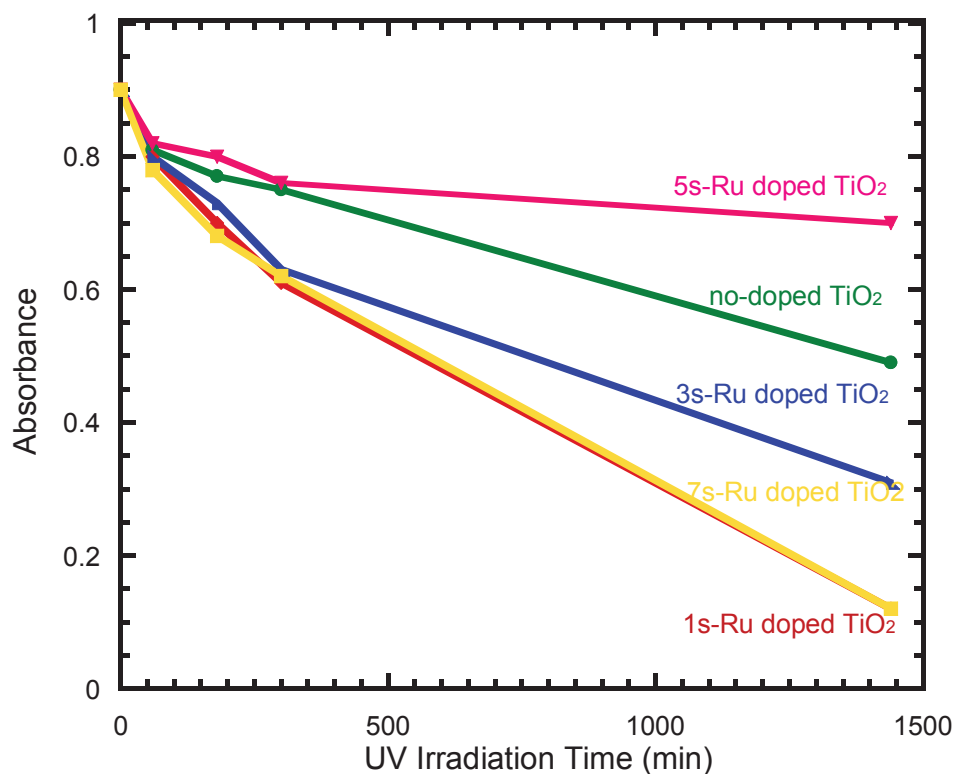


Figure 4.21. Absorbance decay of Methylene Blue (MB) solution & UV irradiation time for the undoped and Ru- doped TiO₂ thin films

Figure 4.21 was created using the top points of absorbance value previously photocatalytic degradation graphs. As can be seen from the Figure 4.21., 1s-Ru doped TiO₂ and 7s-Ru doped TiO₂ absorbance values gradually decreased with increasing time. After 24 hours, undoped TiO₂ and all Ru-doped TiO₂ did not reach to zero values of absorbance. This means that methylene blue solution has not become completely colorless. Its colour changed from dark blue to light blue slightly end of the 24 hours.

A curve between $\ln(A_0/A)$ versus UV-irradiation time was formed according to the equation before. From this curve, the rate constant (k) in (min.)⁻¹ are given in Table 4.3. From this table, (k) value of 1s-Ru doped TiO₂ thin film has higher value among other.

According to the equation, (k) value increases with the decreasing of absorbance (A) value after irradiated UV light. When (k) value increased, photocatalytic activity was increased. Hereby, 1s-Ru doped TiO₂ thin film has higher photocatalytic activity than other prepared thin films.

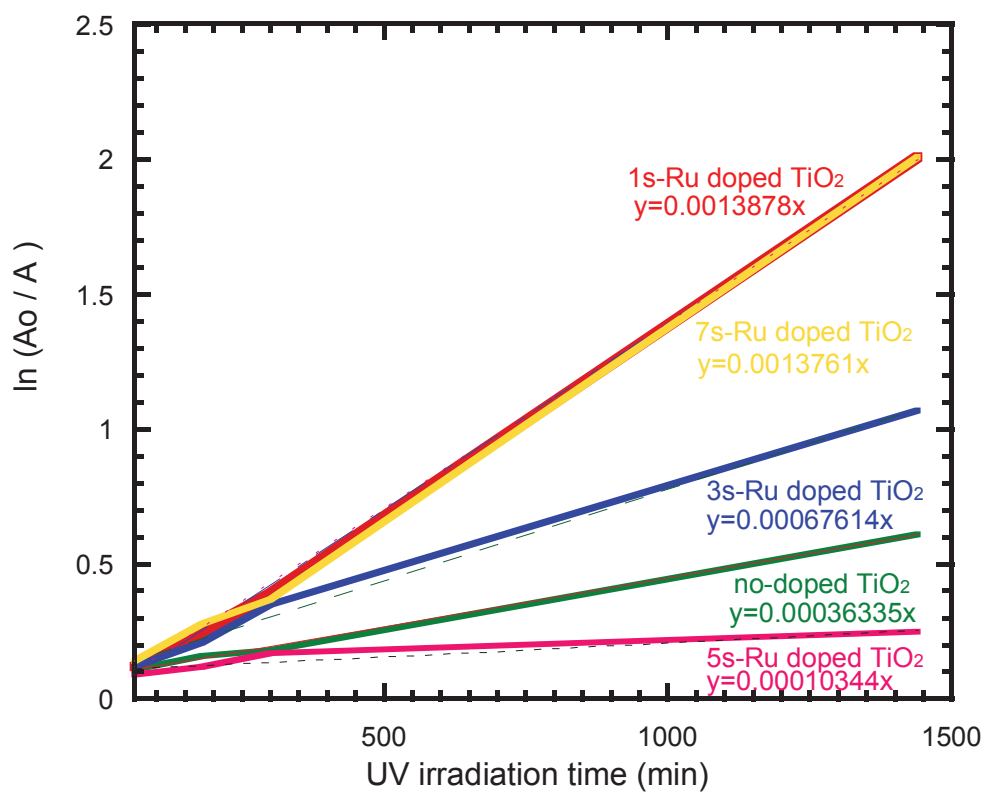


Figure 4.22. $\ln (A_0 / A)$ versus UV irradiation time for the undoped and Ru-doped TiO_2 thin films

Table 4.4. The values of $k \text{ (min)}^{-1}$ prepared Thin Films

Thin Film Sample	The values of $(k) \text{ (min.)}^{-1}$
Undoped TiO_2 thin film	0.00036335
1 s- Ru doped TiO_2 thin film	0.0013878
3s- Ru doped TiO_2 thin film	0.00067614
5s- Ru doped TiO_2 thin film	0.00010344
7s- Ru doped TiO_2 thin film	0.0013761

CHAPTER 5

CONCLUSION

In this thesis, the main purpose was to investigate the influence of optical qualities of different varieties of Ru⁺ doped TiO₂ thin films on their photocatalytic activity. This obtained thin film could be used top of the solar panel surface without inhibition any solar radiation thanks to hydrophilic, self-cleaning, effortless, non-toxic and low-cost properties. D.C. Magnetron Sputtering Technique was used for deposition of thin films. This technique allows the controlling of the thin film structure by changing the deposition parameters.

In this thesis, different percentages of undoped and ruthenium doped TiO₂ thin film photocatalysts were produced on soda lime glasses (SLG) by magnetron sputtering technique. Firstly, coating parameters such as coating time, thickness, the gas amount used were optimized on thin film structure, optical and photocatalytic properties were investigated. After the necessary coating optimizations were completed, heat treatment was performed at 500 °C. After thermal treatments at high temperatures, there is no cracking was observed in the coatings, which indicates the mechanical strength of the thin film formed. Optical and morphological characterization techniques of thin films were performed after heat treatment. The following results were obtained in accordance with the studies carried out.

In the photocatalytic activity tests, the methylene blue solution used as an organic impurity was found to be degraded under UV light. The degradation reaction of low concentrations of methylene blue solution corresponds to the first degree of the speed laws as stated in the literature.

The transmission of Ru⁺ doped TiO₂ coated SLG higher than 70%. The most significant increase in transmission occurred in the spectral range between 450nm - 550nm. Our main purpose to maintain absorption of solar panel and we obtained that sufficient ratio of transmission.

According to XRD results, the anatase phase was obtained 1s Ru-doped and 7s Ru-doped of TiO₂ thin films. 1s and 7s Ru doped TiO₂ thin film had the highest

photocatalytic activity under ultraviolet light, photocatalytic activity varies according to the amount of Ru⁺ doped and the undoped TiO₂ thin film had the lowest photocatalytic activity under ultraviolet light. In this way, they were good at self-cleaning performance. These results prove that the two experiments were overlapped to each other.

When the SEM analysis images of undoped TiO₂ and Ru⁺-doped TiO₂ are examined morphologically, it was seen that the surfaces were similar in structure and a film layer which did not generally have a very rough structure was obtained.

To determine whether the doped Ru⁺ ions settle into the TiO₂ or not in the crystal structure, after the SEM analysis of the thin film, the EDX method was used for elemental analysis. EDX analyses were performed in a selected region on SEM images and the results were obtained as a mean % value. Ru⁺ metal ions doping in all analyzes were determined in TiO₂ crystal structure.

As seen from the results of photocatalytic activity, it was determined that the photocatalytic activity of Ru⁺ ion doped TiO₂ coated surfaces with significantly increased compared to the activity of undoped TiO₂ coated surfaces.

After light irradiation, it enables the effective separation of the positive holes which is formed in the valence band by moving of the electron into the conduction band with the effect of Ru⁺ ion. These positive holes in the Ru⁺ ion allow the formation of hydroxyl radicals from the hydroxide ions adsorbed on the catalyst surface. These radicals are known to act as highly effective oxidants. The reaction of positive holes with Ru⁺ ion inhibits the recombination of the e⁻_{CB} h⁺_{VB} pair, resulting in increased photocatalytic activity.

REFERENCES

- AbdulHussain A., Al-Khafaji, K., (2016). Photocatalysis of Sol-Gel Derived (TiO_2) For Anti-Dust Properties Physics, University of Baghdad Ph.D. thesis, 1-140.
- Adachi, T., Sanjay S. L., Suresh, W. G., Nitish, R., N, S., Hiroshi, I., Kazuki, K., (2018). Photocatalytic, Superhydrophilic, Self-Cleaning TiO_2 Coating on Cheap, Light-Weight, Flexible Polycarbonate Substrates. *Applied Surface Science*, 458-917–23.
- Akhavan, O., (2009). Lasting Antibacterial Activities of $\text{Ag-TiO}_2/\text{Ag/a-TiO}_2$ Nanocomposite Thin Film Photocatalysts under Solar Light Irradiation. *Journal of Colloid and Interface Science*, 336 (1): 117–24.
- Bakardjieva, S., and Nataliya, M., (2009). Applied Catalysis B : Environmental Efficient Gas Phase Photodecomposition of Acetone by Ru-Doped Titania. *Applied Catalysis B Environmental*, 89(3-4): 613–19.
- Banerjee, S., Dionysios, D. D., Suresh, C. P., (2015). Environmental Self-Cleaning Applications of TiO_2 by Photo-Induced Hydrophilicity and Photocatalysis. *Applied CatalysisB,Environmental*, 176–177: 396–428.
- Beeldens, A., (2006). An Environmental Friendly Solution for Air Purification and Self-Cleaning Effect: The Application of TiO_2 as Photocatalyst in Concrete. Tra - Transport Research Arena Europe: Goeteborg, Sweden, June 12th-15th Greener, Safer and Smarter Road Transport for Europe Proceedings, TRBAM,01102613.
- Benedix, R., Frank, Dehn., Jana, Quaas., and Marko, O., (2000). Application of Titanium Dioxide Photocatalysis to Create Self-Cleaning Building Materials. *Lacer*, 5: 157–68.

- Berger, H., Tang, H., and Lévy, F. (1993). Growth and Raman Spectroscopic Characterization of TiO₂ Anatase Single Crystals. *Journal of Crystal Growth*, 130 (1–2): 108–12.
- Berger, T., Sterrer, M., Diwald, O., Knözinger, E., Panayotov, D., Thompson, T. L., and Yates, J. T., (2005). Light-Induced Charge Separation in Anatase TiO₂ Particles. *Journal of Physical Chemistry B*. 109 (13): 6061–68.
- Bouhadoun, S., Guillard, C., Sorgues, S., Hérissan, A., Colbeau-Justin, C., Dapozze, F., Habert, Aurélie., Maurel, V., Herlin-Boime, N., (2017). Laser Synthesized TiO₂-Based Nanoparticles and Their Efficiency in the Photocatalytic Degradation of Linear Carboxylic Acids. *Science and Technology of Advanced Materials*, 18 (1): 805–15.
- Carp, O., Huisman, C. L., and Reller., (2004). Photoinduced Reactivity of Titanium Dioxide. *Progress in Solid State Chemistry*, 32 (1–2): 33–177.
- Centi, G., and Perathoner, S., (2014). Advanced Oxidation Processes In Water Treatment Gabriele. *Handbook of Advanced Methods And Processes in Oxidation Catalysis*, 251-290.
- Chan, C., Man Kin Fung, A., Mu Yao Guo, H., Djurišić, A. B., Leung, F., and Chan, Wai Kin., (2013). Antibacterial and Photocatalytic Activities of TiO₂ Nanotubes. *Journal of Experimental Nanoscience*, 8 (6): 695–703.
- Chang, X., Gong, J., Chang, T., Wang, X., and Gong, J., (2017). Effective Charge Carrier Utilization in Visible-Light-Driven CO₂ Conversion. *Semiconductors and Semimetals*, 97.
- Chemin, J., Bulou, S., Baba, K., Fontaine, C., Sindzingre, T., Boscher, N. D., Choquet, P., (2018). Transparent Anti-Fogging and Self-Cleaning TiO₂/SiO₂ thin Films on Polymer Substrates Using Atmospheric Plasma. *Scientific Reports* 8 (1): 1–8.

- Chen, C., Lin, J. S., Diao, E., and Liu, T. F., (2008). Self-Cleaning Characteristics on a Thin-Film Surface with Nanotube Arrays of Anodic Titanium Oxide. *Applied Physics A: Materials Science and Processing*, 92 (3): 615–20.
- Chen, X., Mao, S. S., (2007). Titanium Dioxide Nanomaterials : Synthesis , Properties , Modifications , and Applications. *Chem. Rev.*107(7): 2891-2959.
- Chen, X., Shen, S., Guo, L., S. Mao, S., (2010). Semiconductor-Based Photocatalytic Hydrogen Generation. *Chemical Reviews*, 110 (11): 6503–70.
- Cristóbal L., Belén, A., Vega, A. M., and López, A. L., (2012). Next Generation of Photovoltaics. *Springer Series in Optical Sciences*, 642-23369-2.
- Darwish, Z. A., Kazem, H. A., Sopian, K., Alghoul, M. A., and Chaichan, M. T., (2013). Impact of Some Environmental Variables with Dust on Solar Photovoltaic (PV) Performance: Review and Research Status. *Researchgate.Net*, 7 (4): 152–59.
- Daude, N., Gout, C., and Jouanin, C., (1977). Electronic Band Structure of Titanium Dioxide. *Physical Review B*, 15 (6): 3229–35.
- Dhayal, M., Jun, Ji., Gu, H. B., and Park, K. H., (2007). Surface Chemistry and Optical Property of TiO₂ Thin Films Treated by Low-Pressure Plasma. *Journal of Solid State Chemistry*, 180 (10): 2696–2701.
- Dumitriu, D., Bally, A. R., Ballif, C., Hones, P., Schmid, P. E., Sanjinés, R., Lévy, F., Pârvulescu, V. I., (2000). Photocatalytic Degradation of Phenol by TiO₂ Thin Films Prepared by Sputtering. *Applied Catalysis B: Environmental*, 25 (2–3): 83–92.
- Etacheri, V., Valentin, C., and Schneider, J., (2015). Visible-Light Activation of TiO₂ Photocatalysts : Advances in Theory and Experiments. *Journal of Photochemistry and Photobiology C: Photochemistry Reviews*, 25: 1-29.

- Faisal, I., Ghoshal, A., (2000). Removal of Volatile Organic Compounds from Polluted Air. *Journal of Loss Prevention in the Process Industries* 13 (13): 527–45.
- Gamage, J., and Zhang, Z., (2010). Applications of Photocatalytic Disinfection. *International Journal of Photoenergy*, 764870:1-11.
- Gnaser, H., Huber, B., Ziegler, C., (2004). *Nanocrystalline TiO₂ for Photocatalysis*. Vol.6.
- Gomes, D., Nara, J. C., De Souza, C., and Josmary, R. S., (2013). Using a Monocular Optical Microscope to Assemble a Wetting Contact Angle Analyser. *Measurement: Journal of the International Measurement Confederation*, 46 (9): 3623–27.
- Gu, Q., Long, J., Fan, L., Chen, L., Zhao, L., Lin, H., and Wang, X., (2013). Single-Site Sn-Grafted Ru / TiO₂ Photocatalysts for Biomass Reforming: Synergistic Effect of Dual Co-Catalysts and Molecular Mechanism. *Journal of Catalysis*, 303: 141–55.
- Guo, S., Wu, Z., and Zhao, W., (2009). TiO₂-Based Building Materials: Above and beyond Traditional Applications. *Chinese Science Bulletin*, 54 (7): 1137–42.
- Gurr, J. R., Wang, A., Chen, C. H., and Yan, Kun., (2005). Ultrafine Titanium Dioxide Particles in the Absence of Photoactivation Can Induce Oxidative Damage to Human Bronchial Epithelial Cells. *Toxicology*, 213 (1–2): 66–73.
- Gutiérrez, M. P., Li, H., and Patton, J., (2002). Thin Film Surface Resistivity In Partial Fulfillment of Course Requirements for Mate-210. *Experimental Methods in Materials Engineering Fall by Professor G. Selvaduray*, 0–24.
- Hamzah, N., Nordin, N. M., Nadzri, A. H. A., Nik, Y. A., Kassim, M. B., and Yarmo, M. A., (2012). Enhanced Activity of Ru/TiO₂ Catalyst Using Bisupport, Bentonite-TiO₂ for Hydrogenolysis of Glycerol in Aqueous Media. *Applied Catalysis A: General*, 419–420: 133–41.

- Hashimoto, K., Irie, H., and Fujishima, A., (2005). TiO₂ Photocatalysis: A Historical Overview and Future Prospects. *Japanese Journal of Applied Physics, Part 1: Regular Papers and Short Notes and Review Papers*, 44 (12): 8269–85.
- He, C., Li, X. Z., Graham, N., and Wang, Y., (2006). Preparation of TiO₂/ITO and TiO₂/Ti Photoelectrodes by Magnetron Sputtering for Photocatalytic Application. *Applied Catalysis A: General*, 305 (1): 54–63.
- Heerden, J., Van, L., and Swanepoel, R., (1997). XRD Analysis of ZnO Thin Films Prepared by Spray Pyrolysis. *Thin Solid Films*, 299 (1–2): 72–77.
- Herrmann, J. M., (1999). Heterogeneous Photocatalysis: Fundamentals and Applications to the Removal of Various Types of Aqueous Pollutants. *Catalysis Today*, 53 (1): 115–29.
- Houas, A., Lachheb, H., Ksibi, M., Elaloui, E., Guillard, Chantal., and Herrmann. Jean-marie., (2001). Photocatalytic Degradation Pathway of Methylene Blue in Water, *Applied Catalysis B Environmental* 31(2): 145–57.
- Ibhadon, A. O., and Fitzpatrick, P., (2013). Heterogeneous Photocatalysis: Recent Advances and Applications. *Catalysts*, 3(1):189–218.
- Indian Institute of Science (Bangalore), Vinu, and Giridhar, M., (1914). *Journal of the Indian Institute of Science*. Vol. 90.
- Isaifan, R. J., Samara, A., Suwaileh, W., Johnson, D., Yiming, W., Abdallah, A. A., and Aïssa, B., (2017). Improved Self-Cleaning Properties of an Efficient and Easy to Scale up TiO₂ Thin Films Prepared by Adsorptive Self-Assembly. *Scientific Reports*, 7 (1): 1–9.
- Jameel, L. Z. N., Haider, A. J., and Taha, S. Y., (2013). Synthesis of TiO₂ Nanoparticles by Using Sol-Gel Method and Its Applications as Antibacterial Agents. *Eng. & Tech. Journal*, 32, 1–10.

- Jung, S. C., Kim, S. J., Imaishi, N., Cho, Y. I., (2005). Effect of TiO₂ Thin Film Thickness and Specific Surface Area by Low-Pressure Metal-Organic Chemical Vapor Deposition on Photocatalytic Activities. *Applied Catalysis B: Environmental*, 55 (4): 253–57.
- Kaldellis, J. K., Fragos, P., Kapsali, M., (2011). Systematic Experimental Study of the Pollution Deposition Impact on the Energy Yield of Photovoltaic Installations. *Renewable Energy*, 36 (10): 2717–24.
- Kaldellis, J. K., and Kokala A., (2010). Quantifying the Decrease of the Photovoltaic Panels' Energy Yield Due to Phenomena of Natural Air Pollution Disposal. *Energy*, 35 (12): 4862–69.
- Karunagaran, B., Kim, Kyunghae., Mangalaraj, D., Yi, Junsin., and Velumani. S., (2005). Structural, Optical and Raman Scattering Studies on DC Magnetron Sputtered Titanium Dioxide Thin Films. *Solar Energy Materials and Solar Cells* 88 (2): 199–208.
- Kasim, N.K., Al-Wattar, A.J., and Abbas, K.K., (2010). New Technique for Treatment of the Dust Accumulation from PV Solar Panels Surface. *Iraqi Journal of Physics*, 8(12): 54–59.
- Kathirvelu, S., D'Souza, L., Dhurai, B., (2008). Nanotechnology Applications in Textiles. *Indian Journal of Science and Technology*, 1 (5).
- Khan M.M., Adil S.F., Al-Mayouf A. Metal oxides as photocatalysts. *J. Saudi Chem. Soc*, 19:462–464.
- Kikuchi, Y., Sunada, K., Iyoda, T., and Hashimoto, K., (1997). Photocatalytic bactericidal effect of TiO₂ Thin films dynamic view. *Journal of Biomaterials and Nanobiotechnology*, 106: 51–56.
- Kopidakis, N., (2013). Time-Resolved Microwave Conductivity, TiO₂ Photoreactivity and Size Quantization, *J. Chem. Soc. Faraday Trans.* 90 (21): 3315-3322.

- Köseğlu, H., Türkoğlu, F., Kurt, M., Yaman, M. D., Akça, F. G., Aygün, G., and Özyüzer, L. (2015). Improvement of optical and electrical properties of ITO thin films by electro-annealing. *Vacuum*, 120, 8-13.
- Kubacka, A., Suárez Diez, M., Rojo, D., Bargiela, R., Ciordia, S., Zapico, I., Albar, J. P., (2014). Understanding the Antimicrobial Mechanism of TiO₂-Based Nanocomposite Films in a Pathogenic Bacterium. *Scientific Reports* 4: 1–9.
- Li, R., Li. C., (2017). Photocatalytic Water Splitting on Semiconductor-Based Photocatalysts. *Advances in Catalysis*, *Advances in Catalysis*, 0360-0564.
- Lisi, D., (2002). Self -cleaning glass, *Universita Degli Studi di Lecce, Corso di Laurea in Ingegneria dei Materiali*, 1–29.
- Luo, S., Vovchok, D., Llorca, J., Sallis, S., Kattel, S., Xu, W., Piper, L. F. J., Polyansky, D. E., Rodriguez. A., (2016). Three-Dimensional Ruthenium-Doped TiO₂ Sea Urchins for Enhanced Visible-Light-Responsive H₂ Production, *Physical Chemistry Chemical Physics*, 15972–79.
- Macwan, D. P., Balasubramanian, C., Dave, P.N., and Chaturvedi, S., (2014). Thermal Plasma Synthesis of Nanotitania and Its Characterization. *Journal of Saudi Chemical Society*, 18 (3): 234–44.
- Malati, M. A., (2010). The Photocatalysed Removal of Pollutants from Water. *Environmental Technology*, 16: 1093-1099
- Masuko, K., Shigematsu, M., Hashiguchi, T., Fujishima, D., Kai, M., Yoshimura, N., Yamaguchi, T., (2014). Achievement of More than 25% Conversion Efficiency with Crystalline Silicon Heterojunction Solar Cell. *IEEE Journal of Photovoltaics*, 4 (6): 1433–35.
- Mo, J., Zhang, Y., Xu, Q., Lamson, J. J., Zhao. R., (2009). Photocatalytic Purification of Volatile Organic Compounds in Indoor Air: A Literature Review. *Atmospheric Environment*, 43 (14): 2229–46.

- Nam, H. J., Amemiya, T., Murabayashi, M., Itoh, K., (2004). Photocatalytic Activity of Sol-Gel TiO₂ Thin Films on Various Kinds of Glass Substrates: The Effects of Na⁺ and Primary Particle Size. *Journal of Physical Chemistry B*, 108 (24): 8254–59.
- Navrotsky, A., Jamieson, J. C., and Kleppa, O. J., (2008). Enthalpy of Transformation of a High-Pressure Polymorph of Titanium Dioxide to the Rutile Modification. *American Association for the Advancement of Science*, 158 (3799): 388–89.
- Nishimoto, S., and Bhushan, B., (2013). Bioinspired Self-Cleaning Surfaces with Superhydrophobicity, Superoleophobicity, and Superhydrophilicity. *RSC Advances*, 3 (3): 671–90.
- Nukaya, Y., Krishna, K. M., Jimbo, T., Soga, T., and Umeno, M., (2002). Photovoltaic and Spectral Photoresponse Characteristics of N-C/p-C Solar Cell on a p-Silicon Substrate. *Applied Physics Letters*, 77 (10): 1472–74.
- Ohama, Y., Gemert, D. V., (2011). Applications of Titanium Dioxide Photocatalysis to Construction Materials. *RILEM State of the Art Reports*, 978-94-007-1297-3.
- Ohno, T., Tanigawa, F., Fujihara, K., Izumi, S., and Matsumura, M., (1999). Photocatalytic Oxidation of Water by Visible Light Using Ruthenium-Doped Titanium Dioxide Powder. *Journal of Photochemistry and Photobiology A Chemistry*, 127 (1-3): 107–10.
- Ozdemir, M., Kurt, M., Ozyuzer, L., and Aygun, G. (2016). Comparison of Photocatalytic Properties of TiO₂ Thin Films and Fibers. *The European Physical Journal*, 1–6.
- Pan, H., Zhu, S., Lou, X., Mao, L., Lin, J., Tian, F., Zhang, D., (2015). Graphene-Based Photocatalysts for Oxygen Evolution from Water. *RSC Advances*, 5 (9): 6543–52.
- Pan, J., Liu, G., (2017). Facet Control of Photocatalysts for Water Splitting. *Semiconductors and Semimetals*. Elsevier Inc, 1st ed. Vol. 97.

- Panayotov, D. A., and Morris, J. R., (2009). Thermal Decomposition of a Chemical Warfare Agent Simulant (DMMP) on TiO₂: Adsorbate Reactions with Lattice Oxygen as Studied by Infrared Spectroscopy. *Journal of Physical Chemistry C*, 113 (35): 15684–91.
- Peerakiathajohn, P., Onreabroy, W., Chawengkijwanich, C., and Chiarakorn, S., (2011). Preparation of Visible-Light-Responsive TiO₂ Doped Ag Thin Film on PET Plastic for BTEX Treatment. *Journal of Sustainable Energy & Environment*, 2: 121–25.
- Pelizzetti, E., and Minero, C., (2012). Comments on Inorganic Chemistry : A Journal of Critical Discussion of the Current Literature Metal Oxides as Photocatalysts for Environmental Detoxification, *Comments on Inorganic Chemistry*, 15: 297–337.
- Rossi, M., (2001). *Crystal Structure Determination by Werner Massa*. (English Translation by R. O. Gould.) Heidelberg: Springer-Verlag. Pp. Xi + 206. Price (Soft Cover) DM 69.00. ISBN 3-540-65970-6. *Acta Crystallographica Section B Structural Science*, 57 (3): 440–440.
- Sankar, S., and Gopchandran, K. G., (2009). Effect of Annealing on the Structural, Electrical and Optical Properties of Nanostructured TiO₂ Thin Films. *Crystal Research and Technology*, 44 (9): 989–94.
- Schneider, H., Niegisch, N., Mennig, M., and Schmidt, H., (2012). Hydrophilic Coating Materials.” *Sol-Gel Technologies for Glass Producers and Users*, 187–94.
- Schroder, K. D., (2005). *Semiconductor Material and Device Characterization*, Third Edition, 978-0-471-73906-7.
- Senthilnathan, M., Ho, D. P., Vigneswaran, S., Ngo, H. H., and Shon, H. K., (2010). Visible Light Responsive Ruthenium-Doped Titanium Dioxide for the Removal of Metsulfuron-Methyl Herbicide in Aqueous Phase. *Separation and Purification Technology*, 75 (3): 415–19.

- Serpone, N., Lawless, D., and Khairutdinov, R., (2005). Size Effects on the Photophysical Properties of Colloidal Anatase TiO₂ Particles: Size Quantization versus Direct Transitions in This Indirect Semiconductor. *The Journal of Physical Chemistry*, 99 (45): 16646–54.
- Sims, R. A., Biris, A. S., Wilson, J. D., Yurteri, C. U., Mazumder M.K., Calle, C. J., Buhler, C. R. (2000). Development of a Transparent Self-Cleaning Dust Shield for Solar Panels. *Proceedings of the First Joint Meeting IEEE-IAS and Electrostatics Society of America (ESA)*, 1: 814–21.
- Skaaland, A., Ricke, M., Wallevik, K., Strandberg, R., Imenes, A., (2011). Potential and Challenges for Building Integrated Photovoltaics in the Agder Region. *Agderforskning, Technical Report*, 6/2011: 1–120.
- Štangar, U., Lavrenčič, N., Tušar, N., Šuligoj, A., Verhovšek, D., Ristić, A., and Mazaj, M., (2015). TiO₂–SiO₂ Films from Organic-Free Colloidal TiO₂ Anatase Nanoparticles as Photocatalyst for Removal of Volatile Organic Compounds from Indoor Air. *Applied Catalysis B: Environmental*, 184: 119–31.
- Stathatos, E., Petrova, T., Lianos, P., (2001). Study of the Efficiency of Visible-Light Photocatalytic Degradation of Basic Blue Adsorbed on Pure and Doped Mesoporous. *Titania Films*, 14: 5025–30.
- Sze, M. S., (2002). *Semiconductor Devices, Physics and Technology. Semiconductor Devices Physics Technology 2nd Ed.*
- Tada, H., (1997). Dependence of TiO₂ Photocatalytic Activity upon Its Film Thickness. *Langmuir*, 21: 360–64.
- Tang, H., Prasad, K., Sanjinès, R., Schmid, P.E., and Lévy, F., (1994). Electrical and Optical Properties of TiO₂ anatase Thin Films. *Journal of Applied Physics*, 75 (4): 2042–47.

- Tauc, J., and Menth. A., (1972). States in the Gap, *Journal of Non-Crystalline Solids*, 8–10 (C): 569–85.
- Tiefeng, Xu., Feifei, C., Shixun, D., Qiuhua, N., Xiang, S., and Xunsi, W., (2009). Third-Order Optical Nonlinear Characterizations of Bi₂O₃-B₂O₃-TiO₂ Ternary Glasses. *Physica B: Condensed Matter* 404 (14–15): 2012–15.
- Ulucan, S., Aygun, G., Ozyuzer, L., Egilmez, M., Turan, R., (2005). Properties of Reactive O₂ Ion Beam Sputtered TiO₂ on Si Wafers. *Journal of Optoelectronics and Advanced Materials*, 7: 297-300.
- Vernardou, D., Kalogerakis G., Stratakis E., Kenanakis G., Koudoumas, E., Katsarakis, Nikos. (2009). Photoinduced Hydrophilic and Photocatalytic Response of Hydrothermally Grown TiO₂ Nanostructured Thin Films. *Solid State Sciences*, 11 (8): 1499–1502.
- Vonderhaar, G., (2017). Efficiency of Solar Cell Design and Materials. *Missouri S&T's Peer to Peer*, 1-2.
- Wang, Y., Sun, C., Zhao, X., Cui, B., Zeng, Z., Wang, A., Liu, G., Cui, H., (2016). The Application of Nano-TiO₂ Photo Semiconductors in Agriculture. *Nanoscale Research Letters*, 11 (1): 1–7.
- World Energy Statistics|Enerdata. (2019). *Global Energy Statistical Yearbook*, (Accessed April 15, 2019). <https://yearbook.enerdata.net/>.
- Yao, L., and He, J., (2014). Recent Progress in Antireflection and Self-Cleaning Technology From Surface Engineering to Functional Surfaces. *Progress in Materials Science*, 61: 94–143.
- Zou, Y., Gong, Y., Lin, B., and Mellott, N. P., (2016). Photodegradation of Methylene Blue in the Visible Spectrum: An Efficient W⁶⁺ Ion Doped Anatase Titania Photocatalyst via a Solvothermal Method. *Vacuum* 126: 63–69.